STARS

University of Central Florida
STARS

Electronic Theses and Dissertations, 2004-2019

2015

A Binary Approach for Selective Recognition of Nucleic Acids and Proteins

Evan Cornett
University of Central Florida

 Part of the Biology Commons
Find similar works at: https://stars.library.ucf.edu/etd
University of Central Florida Libraries http://library.ucf.edu

This Doctoral Dissertation (Open Access) is brought to you for free and open access by STARS. It has been accepted for inclusion in Electronic Theses and Dissertations, 2004-2019 by an authorized administrator of STARS. For more information, please contact STARS@ucf.edu.

STARS Citation
Cornett, Evan, "A Binary Approach for Selective Recognition of Nucleic Acids and Proteins" (2015). *Electronic Theses and Dissertations, 2004-2019*. 1483.
https://stars.library.ucf.edu/etd/1483

A BINARY APPORACH FOR SELECTIVE RECOGNITION OF NUCLEIC ACIDS AND PROTEINS

by

EVAN M. CORNETT
B.S. University of Central Florida, 2009
M.S. University of Central Florida, 2012

A dissertation submitted in partial fulfillment of the requirements
for the degree of Doctor of Philosophy
in the Department of Biology
in the College of Science
at the University of Central Florida
Orlando, Florida

Spring Term
2015

Major Professor: Dmitry M. Kolpashchikov

© 2015 Evan M. Cornett

ABSTRACT

The design of probes for the selective recognition of biopolymers (nucleic acids and proteins) is a fundamental task for studying, diagnosing, and treating diseases. Traditional methods utilize a single component (small molecule or oligonucleotide) that binds directly to the target biopolymer. However, many biopolymers are unable to be targeted with this approach. The overarching goal of this dissertation is to explore a new, binary approach for designing probes. The binary approach requires two components that cooperatively bind to the target, triggering a recognition event. The requisite binding of two-components allows the probes to have excellent selectivity and modularity.

The binary approach was applied to design a new sensor, called operating cooperatively (OC) sensor, for recognition of nucleic acids, including selectively differentiating between single nucleotide polymorphisms (SNPs). An OC sensor contains two oligonucleotide probe strands, called O and C, each with two domains. The first domain contains a target recognition sequence, whereas the second domain is complementary to a molecular beacon (MB) probe. Binding of both probe strands to the fully matched analyte generates a full MB probe recognition site, allowing a MB to bind and report the presence of the target analyte. Importantly, we show that the OC sensor selectively discriminates between single nucleotide polymorphisms (SNPs) in DNA and RNA targets at room temperature, including those with stable secondary structures. Furthermore, the combinatorial use of OC sensors to create a DNA logic gate capable of analyzing DNA sequences of *Mycobacterium tuberculosis* is described.

The binary approach was also applied to design covalent inhibitors for HIV-1 reverse transcriptase (RT). In this application, two separate pre-reactive groups were attached to a natural RT ligand, deoxythymidine triphosphate (dTTP). Upon binding of both dTTP analogs in the RT active site, the pre-reactive groups are brought into the proper proximity and react with each other forming an intermediate that subsequently reacts with an amino acid side chain from the RT. This leads to covalent modification of RT, and inhibition of its DNA polymerase activity. This concept was tested *in vitro* using dTTP analogs containing pre-reactive groups derived from β-lactamase inhibitors clavulanic acid (CA) and sulbactam (SB). Importantly, our *in vitro* assays show that CA based inhibitors are more potent than zidovudine (AZT), a representative of the dominant class of RT inhibitors currently used in anti-HIV therapy. Furthermore, molecular dynamics simulations predict that complexes of RT with these analogs are stable, and point to possible reaction mechanisms. The inhibitors described in this work may serve as the basis for the development of the first covalent inhibitors for RT. Moreover, the pre-reactive groups used in this study can be used to design covalent inhibitors for other targets by attaching them to different ligands. Overall, the work presented herein establishes the binary approach as a straightforward way to develop new probes to selectively recognize nucleic acids and proteins.

ACKNOWLEDGMENTS

I am indebted to many people without whom this work would not be possible. First, I acknowledge my advisor, Dmitry Kolpashchikov, Ph.D. I thank him for taking a chance on me. Like the motto of his alma mater, “We will not make your smarter, we will teach you how to think,” he has taught me to think like a scientist. I am very thankful to him for his constant guidance and support.

I am very thankful to the members of my dissertation committee: William T. Self, Ph.D., Debopam Chakrabarti, Ph.D., and Eda Koculi, Ph.D., whose comments, questions, and suggestions have always been helpful. Their critical role in my training is much appreciated. I must also thank Dr. Alexander Balaeff, Ph.D. whom without the Molecular Dynamics portion of this work would have been impossible. His patience and willingness to teach me MD is greatly appreciated.

I am also extremely grateful to all of the support and advice from all of the members of the Kolpashchikov lab, past and present. I am especially grateful to Carlos Ledezma, who was responsible for the synthesis of the reagents used in this work (Chapter 4), Yulia Gerasimova, Ph.D. and Martin O’Steen with whom I collaborated on much of the work presented here, and to Brian Butts for careful reading and suggestions for this manuscript.

I also would like to acknowledge my parents, for always supporting me and pushing me to pursue my dreams. Finally, I want to acknowledge the sacrifice of my wife Lindsey and son Ian. I am so grateful for their love and support. I would not have been able to begin or complete this work without it.

TABLE OF CONTENTS

LIST OF FIGURES

LIST OF TABLES

LIST OF ABBREVIATIONS

AZT	Zidovudine
BDS	Binary DNA sensor
CA	Clavulanic acid
dATP	Deoxyadenosine triphosphate
dCTP	Deoxycytosine triphosphate
ddNTP	Dideoxynucleotide triphosphate
dGTP	Deoxyguanosine triphosphate
DNA	Deoxyribonucleic acid
dNTP	Deoxynucleotide triphosphate
dTTP	Deoxythymidine triphosphate
dUTP	Deoxyuridine triphosphate
DX	Double crossover
HIV	Human immunodeficiency virus
LOD	Limit of detection
M	Mutant
MB	Molecular beacon
Mtb	*Mycobacterium tuberculosis*
NA	Nucleic acid
NNRTI	Non-nucleoside reverse transcriptase inhibitor
NRTI	Nucleoside reverse transcriptase inhibitor
OC	Operating cooperatively
PAGE	Polyacrylamide gel electrophoresis
PCR	Polymerase chain reaction
Rif	Rifampin
RNA	Ribonucleic acid
RT	Reverse transcriptase
SB	Sulbactam
SNP	Single nucleotide polymorphism
TF	2,3,5,6-tetrafluoro-4-hydroxybenzoic acid
WT	Wild-type

CHAPTER 1: GENERAL INTRODUCTION

Proteins and nucleic acids are important biopolymers that perform a wide range of biological functions. The development of probes for the recognition of these biopolymers is a fundamental task for studying, diagnosing, and treating disease. Indeed, substantial efforts have been made to create new probes for this purpose. One of the most important characteristics of a probe is selectivity. Selectivity is the ability of a probe to differentiate its target from non-target molecules, and thus is a range from low (poor) to high (excellent). Traditional methods to develop probes have focused on developing a single ligand designed to selectively recognize the target (Figure 1). This recognition event may report the presence of the target or alter its function. Traditionally, selectivity is achieved by fine-tuning the interaction between the target and ligand. Adjusting chemical groups at different positions to promote high affinity for the target, thus hopefully reducing the likelihood of the probe binding to other biopolymers. Inherently, this limits the degree of selectivity achievable without compromising other important characteristics of the probe. Additionally, the vast majority of the human proteome has yet to be targeted with a probe for research or treatment purposes, perhaps to due limitations of the traditional strategy. Furthermore, a large portion of genomic diversity is due to single nucleotide polymorphism (SNPs), and design of probes for recognition of SNPs is still difficult. Thus, new approaches to design probes for recognition of both proteins and nucleic acids are needed.

Nature's Approach

There are many examples of natural biological systems with distinct and highly selective one-to-one complexes between two partner molecules: antibody-antigen, receptor-ligand, and kinase-substrate. Mimicking this approach to design probes for recognition of nucleic acids and proteins has been successful. However, nature uses more than just the one-to-one approach. Often, recognition events only occur when multiple partners bind to each other. One of the classical examples is the excellent selectivity of sequence specific endonucleases. Structural studies of the an endonuclease from *Escherichia coli* (*E. coli*), EcoRV, revealed an interesting conformational change when EcoRV is bound to its target DNA [1]. EcoRV changes conformations creating a new binding site for the divalent magnesium ions required for cleavage of the target DNA. This conformational change only occurs when EcoRV binds to its target-DNA, allowing this enzyme to perform its function with high selectivity. This classical example illustrates how natural biological systems have evolved to require multiple binding events prior to a recognition event. Inspired by this, we propose a binary approach to design selective probes for recognition of detection of nucleic acids and proteins.

The Binary Approach

This work explores the hypothesis that a binary approach, using two molecules that must simultaneously bind a target biopolymer, will improve selectivity over single-component systems (Figure 1). The general binary scheme requires a target with two

ligand-binding sites adjacent to each other (Figure 2). Two analogs of these ligands are synthesized, each containing an additional function group. When both ligand analogs bind to the target, the additional functional groups are brought in proximity creating a recognition event. This event depends on the functional groups used, but can be generation of a detectable signal or generation of a new group that can alter the activity of the target. In any case, this recognition event only occurs when both ligands correctly bind to the target, increasing the selectivity of the recognition event since random interactions between the two groups in solution is unlikely to occur. Furthermore, it is unlikely that the ligands selected would bind near each other on another target.

It is important to note that all nucleic acids can fulfill the requirement of two adjacent ligand-binding sites. Ligands can be designed to bind to the target at a specific locus through Watson-Crick base pairing. For proteins, ligands that bind at adjacent sites must be available, or efforts must be made to select a new ligand that binds near a known ligand. Fortunately, many enzymes naturally facilitate the binding of multiple small molecules or macromolecules to perform their function, and thus these can be used as ligands to develop a probe following the binary approach. Additionally, enzymes are an important drug class and research area. Indeed, up to 40% of small-molecule drugs target enzymes and an estimated 80% of potential drug targets are enzymes [2,3]. Regardless if the target is protein or nucleic acid, the extra functional group attached to the ligands can vary greatly in its composition. For example, it may consist of an oligonucleotide, reactive small molecule, or a

fluorescent small molecule. Herein, we explore the binary approach to design probes for the selective recognition of nucleic acids and proteins.

Figures and tables

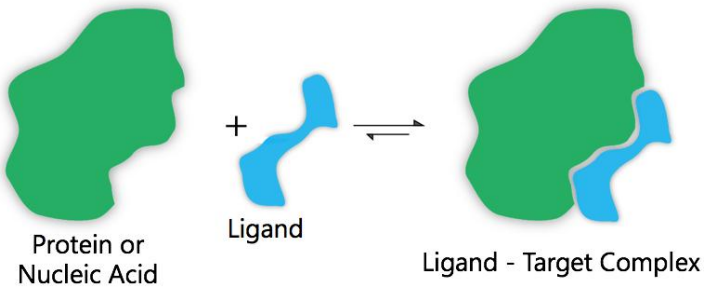

Figure 1. Classical approach to design probes for recognition of nucleic acids or proteins.

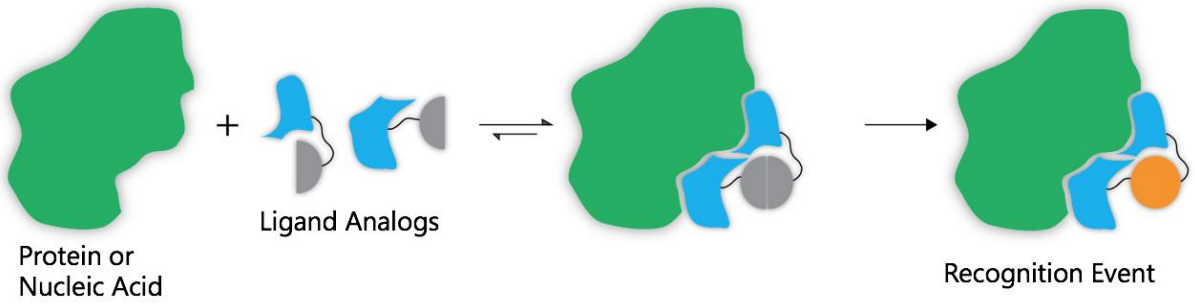

Figure 2. Binary approach to design probes for recognition of nucleic acids or proteins.

In a binary approach, two ligands (blue) are created with additional functional groups (half circles). Upon binding of both ligand analogs to the target, the additional functional groups are facilitated near each other allowing a recognition event to occur.

CHAPTER 2: OPERATING COOPERATIVELY (OC) SENSOR FOR HIGHLY SELECTIVE RECOGNITION OF NUCLEIC ACIDS[†]

Introduction

The analysis of single nucleotide variation in DNA and RNA is important for genotyping of single nucleotide polymorphisms [4,5], somatic mutations [6-8], and methylation changes associated with aging and cancer [9-11]. A molecular beacon (MB) probe [12] is a hybridization sensor that has been extensively utilized for the analysis of single nucleotide variation [13-19]. A traditional MB probe is a stem-loop folded DNA oligonucleotide, with fluorophore and quencher dyes conjugated to opposite ends (Figure 3A). MB probes have found multiple applications in the analysis of biological molecules due to their ability to produce a fluorescent signal instantaneously upon hybridization to complementary nucleic acids. MB probes were found to be more specific towards single base substitutions than linear probes [20-24]. However, in many cases, accurate SNP genotyping still requires elevated temperature and/or measuring melting temperature profiles. Moreover, the design of MB probes remains challenging due to the problems of stem or loop invasion [16,25,26] and poor hybridization with structured sequences [27-31]. Additionally, MB probes are expensive commercial products. The use of a limited number of MB probes for the

[†] Work in this chapter was previously published: Cornett EM, O'Steen MR, Kolpashchikov DM (2013) Operating Cooperatively (OC) sensor for highly specific recognition of nucleic acids. PLoS ONE 8:e55919.

analysis of numerous target sequences is an attractive perspective. In this approach, one, or several, MB probes can be optimized to avoid stem and loop invasion and used as universal sensors for any DNA or RNA analytes (so-called universal MB probes [32]). This approach may enable multiplex genotyping of millions of SNPs in a low budget format. Here we report the design of a sensor that uses a single MB probe to detect multiple nucleic acid sequences.

The sensor has a straightforward design and demonstrates excellent SNP selectivity at ambient temperatures. Additionally, this new sensor is suitable for the analysis of nucleic acids folded in stable secondary structures, such as bacterial 16S rRNA. We have been exploring strategies for indirect binding of an MB probe to specific nucleic acids. The first strategy, binary DNA sensors (BDSs), used two DNA adaptor strands (m and f in Figure 3B). The f and m strands hybridized to both an MB probe and an analyte, forming a DNA four-way junction-like structure (Figure 3B). This approach demonstrated unprecedented selectivity at room temperature [32-34]. The BDS had a straightforward design and enabled detection of stem-loop folded sequences [27,28,34]. The triethylene glycol linkers, situated between the MB-binding and analyte binding arms (dashed lines in Figure 3B) were necessary to promote the stabilization of the DNA four-way junction conformation that produces high fluorescence [32,33]. However, these linkers increased the cost of an adaptor strand by a factor of 5. In an effort to avoid the non-nucleotide modification we explored alternative approaches, which resulted in the design of a double-crossover (DX) tile sensor (Figure 3C) [35,36]. The construct takes advantage of the DX tile, a DNA

structure first investigated by Fu and Seeman [37]. The DX tile sensor consisted of an MB probe, three unmodified DNA adaptor strands (a, b, and c), and an analyte, which together formed a penta-partite complex (Figure 3C). However, the sensor had only moderate selectivity towards a single nucleotide substitution due to the required formation of at least 26 base pairs between the analyte and the adaptor strands. Indeed, long stable hybrids between a probe and a nucleic acid analytes are known to reduce probe selectivity [38]. In an effort to design a nucleic acid sensor that is not cost-prohibitive, yet still maintains excellent SNP selectivity, we report here a new SNP-selective sensor, named ‘operating cooperatively’ or OC sensor (Figure 3D) [39]. In this study, we demonstrate the exceptional SNP selectivity of the OC sensor at room temperature, determine the limit of detection (LOD), and demonstrate how this sensor can be tailored to analyze stem-loop folded DNA and bacterial 16S rRNA.

Materials and Methods

Reagents

All oligonucleotides (sequences listed in Table 1) were custom-made by Integrated DNA Technologies, Inc (Coralville, IA). T7 RNA polymerase, PstI, and NTPs were purchased from New England Biolabs (Ipswich, MA). Chemicals were purchased from Sigma-Aldrich (St. Louis, MO). pEC16SM plasmid was a generous gift from Dr. Dedkova (ASU).

Fluorescence Assay

For the fluorescence assays, UMB1 was added to a buffer containing 50 mM $MgCl_2$, 50 mM Tris-HCl, pH 7.4, at a final concentration of 50 nM. O and C strands, and either matched (rs87T, *E.coli* f1, rs14G) or mismatched (rs87C, *B.sub* f1, rs14A) strands were added to a final concentration of 200 nM, and 500 nM, respectively. Final sample volumes were 120 mL for DNA analytes and 60 mL for bacterial 16S rRNA analytes. For assays with DNA analytes, samples were incubated for 15 minutes at room temperature (22°C). For fluorescence assays with RNA analytes, samples were incubated for 5 minutes in 90°C water bath, followed by 15 minute incubation at room temperature prior to recording fluorescence spectra. Fluorescence spectra were recorded on a Perkin-Elmer (San Jose, CA) LS-55 Luminescence Spectrometer with a Hamamatsu xenon lamp (excitation at 485 nm; emission 517 nm). All experiments were repeated at least three times, and data is shown as the mean with error bars representing one standard deviation from the mean.

Preparation of Bacterial 16S rRNA Analytes

Total RNA was isolated from E. coli (ATCC 8739) and B. subtilis (ATCC 9372) using Omega Biotek Bacterial RNA isolation kit following the manufacture's recommended protocol. Isolated RNA yield was determined, and the presence of 16S rRNA was seen using agarose gel electrophoresis (Figure 5). E. coli 16S rRNA transcript was obtained using in vitro transcription with pEC16SM plasmid, which contains the 16S rRNA gene from E. coli strain A19. PstI was used to linearize

pEC16SM. The in vitro transcription reaction mixture (300 mL) contained linearized pEC16SM (1 mg), NTPs (4 mM each), T7 RNA polymerase in NEB RNA pol reaction buffer supplemented with MgCl2 (20 mM) and bovine serum albumin (25 mg/mL). The reaction was incubated at 37uC for 2 hours. The transcript was collected by ethanol precipitation. The concentration of rRNA transcript was determined by comparison of gel band intensity with gel purified transcript (Figure 4).

Results

The OC sensor uses two unmodified DNA adaptor strands (O and C), each of which binds to a MB probe and a analyte (Figure 3D). The design of the sensor was adjusted to room temperature (22°C). For these conditions, strand O had two 5 or 6 nucleotide MB-binding arms. Thus, the two short binding arms had a very weak interaction with MB probe in the absence of analyte, thus ensuring low fluorescent background. Strand C had 8 or 9 nucleotide MB binding arms; this length was required for the formation of stable DNA four-way junction associates [37]. The analyte binding arm of strand C can be adjusted to provide high mismatch selectivity or stabilization of the OC complex as demonstrated below. Figure 6A shows a design of the OC sensor for the recognition of a human genomic DNA sequence that is known to have a SNP (rs876724). This analyte contains a mutation which has been suggested as a useful marker for human identification in forensic applications [40]. The sensor fluoresced only in the presence of the matched rs87T sequence, but not in the presence of an alternative allele (Figure 6B). The limit of detection (LOD) of the sensor was found to

be 5.5 nM (Figure 7 blue line), which is somewhat above the detection limit of a typical MB probe [12-16,32]. Importantly, the presence of high excess (500 nM) of a single-based substituted analyte did not jeopardize the assay: the cognate analyte was detected with the LOD of 12 nM (Figure 7 red line). Importantly, the LOD is well below the concentration achievable by PCR (~100 nM). In order to demonstrate general applicability of the approach, an OC sensor was designed to recognize an alternative human SNP (rs1490413 Figure 8). Again, the sensor demonstrated excellent SNP discrimination at room temperature. The design of the new sensor was straightforward: (i) the sensor utilized the same MB probe; (ii) only the analyte binding arms of the sensor were changed to complement to the new target.

Natural single stranded nucleic acids are often folded in stable secondary structures. Stable structures prevent hybridization probes, including the MB probe, from interacting with such analytes [27-30,41]. A common approach to overcome this difficulty is to target only unstructured fragments of natural RNAs. This limits the choice of hybridization probes and often prevents analysis of SNPs located in stem regions of such analytes. Here we demonstrate that the OC sensor is capable of analyzing folded nucleic acids. As a model, a fragment of *E. coli* 16S rRNA (*E. coli* f-1 in Figure 9A) was used as a specific analyte and a corresponding fragment of *B. subtilis* 16S rRNA (*B. sub* f-1 in Figure 9A) was used as a non-specific analyte. These analytes were DNA oligonucleotide mimics of the actual RNA sequence. Analysis of 16S rRNA is important for classification of bacteria species and for molecular diagnostics of infectious diseases [42-45]. On the other hand, 16S rRNAs, as well as

their DNA amplicons, can fail to hybridize to oligonucleotide probes [46,47]. In this study, we have randomly selected a fragment of *E. coli* 16S rRNA folded in a typical stemloop structure with a bulge in the middle of the stem (Figure 9A). The predicted melting temperature of this stem was 84.5°C according to IDT Oligo Analyzer software (experimental conditions set at 50 mM $MgCl_2$, 50 mM monocharged ion).

The OC sensor for selective recognition of the stem-loop folded *E. coli* f-1 took advantage of a C2 strand equipped with a long analyte binding arm, containing 30 nucleotides (Figure 9B). The long arm allows the C2 strand to tightly hybridize to an extended portion of the analyte and unwind its secondary structure. However, the long arm may also allow a stable complex to form between C2 and B.sub f-1 analyte. Thus, the O2 strand is designed to contain an analyte binding arm of only 12 nucleotides and will hybridize tightly only to the fully complementary E.coli f1. Indeed, high fluorescence was registered only in the presence of a fully matched strand, but not in the presence of a mismatched B.sub f-1 (Figure 9C).

In order to test the OC sensor against actual bacterial 16S rRNA samples, we used *in vitro* transcription to obtain *E. coli* 16S rRNA. The OC sensor was able to recognize and give high fluorescent signal in the presence of the 16S rRNA transcript (Figure 10A). However, an additional annealing step was required, likely due to a very stable structure of the long 16S rRNA compared to our mimic analytes. Additionally, the OC sensor was applied to the identification of 16S rRNA collected from bacteria samples. The total RNA from *E. coli* and *B. subtilis* was obtained and the OC sensor correctly identified the *E. coli* 16S rRNA. The OC sensor produced a high fluorescence

signal in the presence of *E. coli* RNA, but gave a low signal in the presence of *B. subtilis* RNA or no analyte (Fig. 6B). Thus, the OC sensor is suitable for sequence selective recognition of conformational constrained natural RNAs.

Discussion

MB probes have become an important tool of molecular diagnostics, especially in real-time PCR (rtPCR) format [13,15]. However, the application of MB probes in practice suffers from a number of problems including stem invasion and inability to analyze folded RNA and DNA. Moreover, despite improved selectivity towards mismatched analytes, MB probes still require monitoring of melting profiles for accurate SNP genotyping [13-15]. Multicomponent sensors that use indirect binding of an MB probe to a target DNA or RNA analyte offer a solution for these pitfalls. In this approach, a limited number of optimized MB probes can provide a toolbox for the analysis of millions of human and bacterial SNPs with no need to design a pair of unique MB probes for each new SNP of interest.

Previously, our lab introduced two different designs for MB probe-based multicomponent sensors, each with its respective disadvantages[33,35]. The OC sensor reported here demonstrated marked improvement over the previous designs: it is less expensive than binary DNA sensor and more selective towards SNPs than a DX-tile sensor. Additionally, the OC sensor is suitable for the analysis of secondary structure folded DNA and RNA. Herein, the utility of the OC sensor was demonstrated by adapting an OC sensor for detection of bacterial 16S rRNA. Therefore, the

approach described in this study has potential to become useful for instantaneous detection of nucleic acids in homogeneous solutions. OC sensors used in this study were designed to operate at room temperature to avoid any required temperature control for the hybridization reaction between probes and analyte. However, the design could likely be adjusted to function at elevated temperatures (50–60°C) for applications such as quantitative real time PCR.

The OC sensor produces fluorescent signal instantaneously upon hybridization to a specific nucleic analyte. The MB probe binds to the analyte indirectly, e.g. through two unmodified DNA oligonucleotide adaptor strands. This gives an opportunity to optimize a single MB probe for the analysis of multiple DNA or RNA sequences. The approach provides a versatile tool for nucleic acid analysis at ambient temperature that is SNP specific and capable of analyzing stem-loop folded nucleic acids. Thus the OC sensor represents a promising tool for SNP analysis in homogeneous solution, which might be used for detection and genotyping of bacteria or human SNPs.

Figures and tables

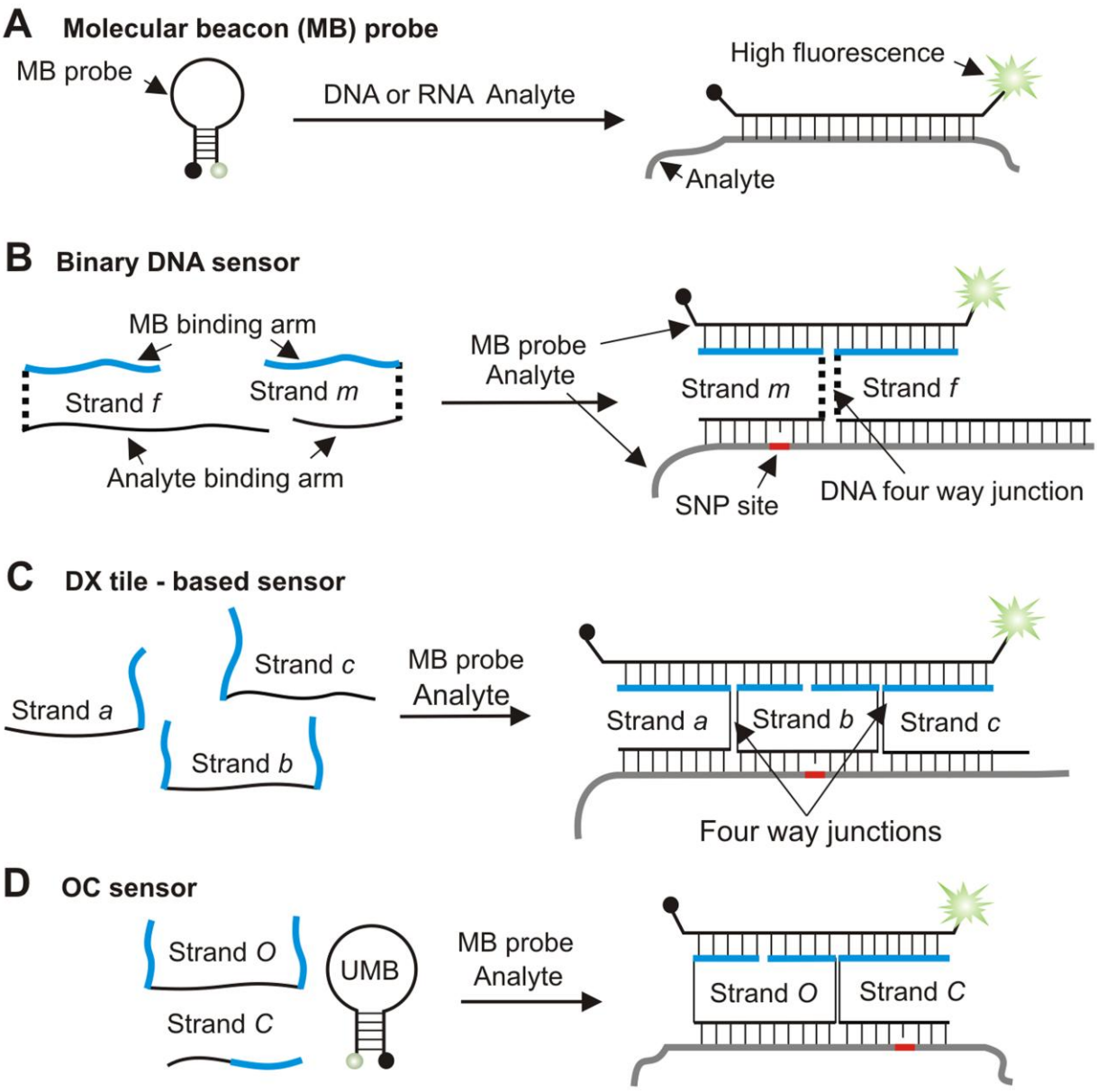

Figure 3. Molecular beacon-based sensors for nucleic acid detection.

A) Conventional MB probe [12].
B) MB-based binary DNA sensor (BDS) [33]. Dashed lines indicate triethylene glycol linkers.
C) DX-tile based sensor [35].
D) OC sensor introduced in this study.

Table 1. Sequences of oligonucleotides used in the OC sensor study.

Name	Sequence	Purification
UMB1	5'-/FAM/CGCGTTAACATACAATAGATCGCG/BHQ1/	HPLC
rs14G	5'-ACTGGGCTGATGTGGGTTCTTTGCAGAACTG GCTGGCCTCAGAGCAGGGA	SD
rs14A	5'-ACTGGGCTGATGTGGGTTCTTTGCAAAACTG GCTGGCCTCAGAGCAGGGACCGCGGCCAGTTCT GCAAAGAACCCACCGCGG	SD
E.coli f-1	5'-TAGTCCGGATTGGAGTCTGCAACTCGACTCC ATGAAGTCGGAAT	SD
B.sub f-1	5'-CAGTTCGGATCGCAGTCTGCAACTCGACTGC GTGAAGCTGGAAT	SD
rs87C	5'-ATACCACTGCACTGAAGTATAAGTACATTTTTT GTCACACTCTGCTAACT	SD
rs87T	5'-ATACCACTGCACTGAAGTATAAGTATATTTTTT GTACACTCTGCTAACT	SD
O1	5'-TATTGTTATACTTCAGTGGCGATC	SD
C1	5'-AATATACTATGTTAACG	SD
O2	5'-TATTGTTCCAATCCGGACGCGATC	SD
C2	5'-ATTCCGACTTCATGGAGTCGAGTTGCAGACA TGTTAACG	SD
O3	5'-TATTGTAAGAACCCACATGCGATC	SD
C3	5'-AGTTCTGCAATGTTAACG	SD

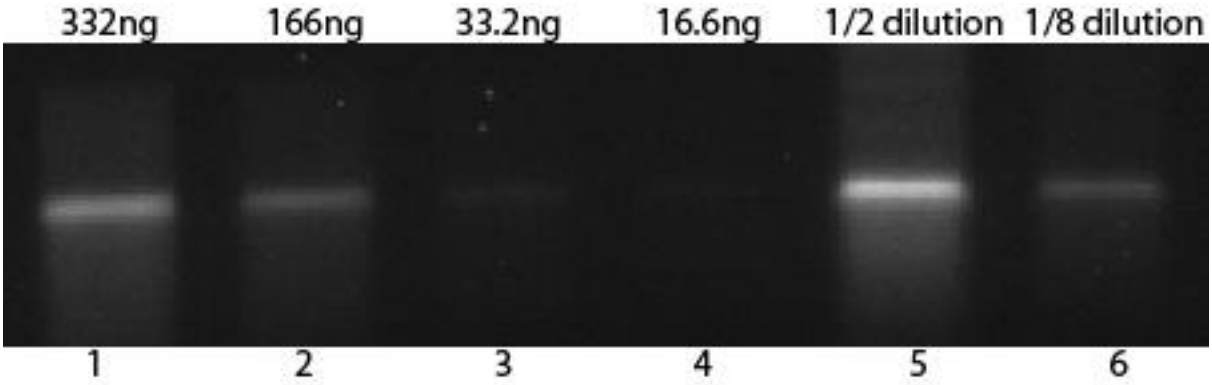

Figure 4. *E. coli* 16S rRNA in vitro transcript concentration was determined using agarose gel electrophoresis.

In vitro *E. coli* 16S rRNA transcript concentration determination by 1% agarose gel electrophoresis with GELRED staining. Transcript was gel purified and concentration determined using a spectrophotometer. Several concentrations of known gel purified transcript (lanes 1–4), as well as 1 µL from two dilutions of unknown concentration used in the fluorescent assays. The 1/8 dilution sample was determined to be equal in intensity to 166 ng band. This was used to determine the concentration of all in vitro transcript samples used in fluorescent assays.

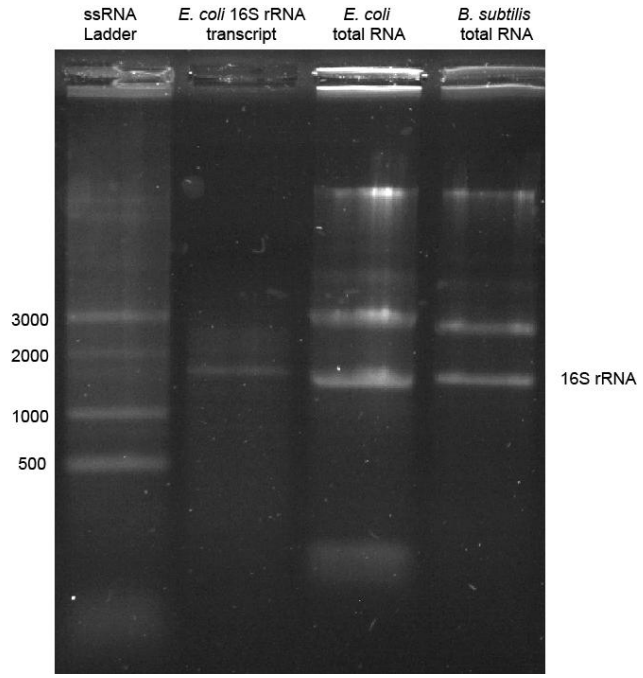

Figure 5. Agarose analysis of total RNA isoltation from *E. coli* and *B. subtilis*.

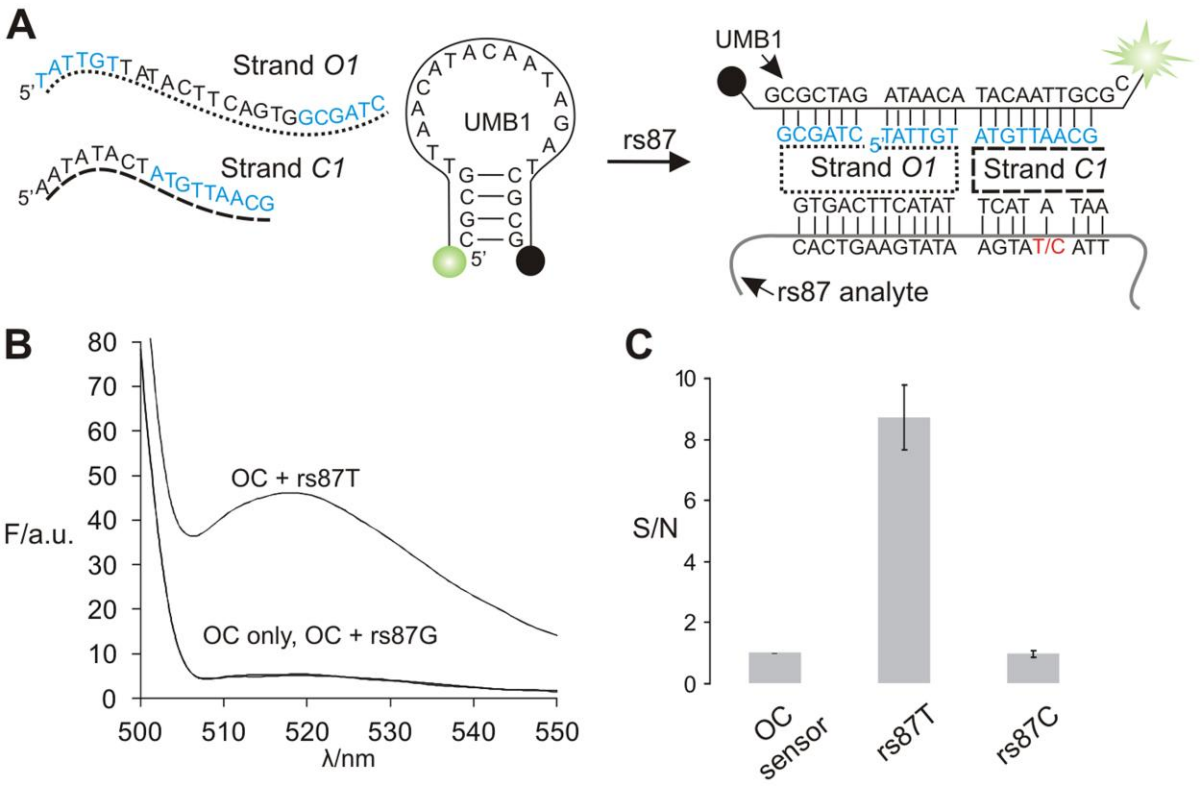

Figure 6. OC sensor selectively recognizes rs876724 SNP T allele.

A) Sensor in complex with rs87T analyte and UMB1 probe. The sensor was designed to recognize the thymidine containing allele, while discriminating against the alternative cytosine containing allele. MB-binding arms are shown in cyan.

B) Fluorescent response of OC sensor specific to rs87T allele sequence in the absence or presence of specific or non-specific analytes.

C) Mean signal-to-noise ratios of four independent experiments with error bars indicating one standard deviation.

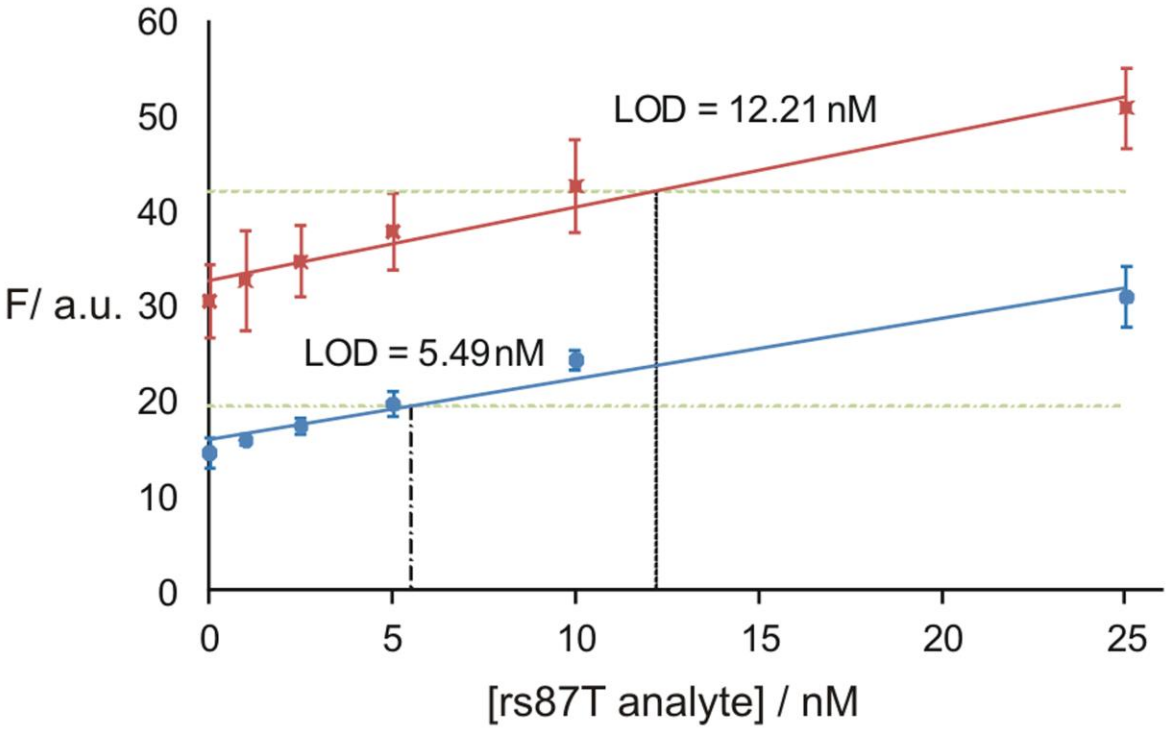

Figure 7. OC sensor limit of detection (LOD).

O1, C1, and UMB1 probe were used to analyze low concentrations of the matched analyte (rs87T). The limit of detection (LOD) was calculated as the analyte concentration that triggered a fluorescent signal equal to the average fluorescence of the background from three independent measurements plus three standard deviations of the average back- ground fluorescence. Data shown were plotted as the mean with error bars representing one standard deviation from the mean from three independent trials. LOD was determined in the absence (blue line) or in the presence (red line) of 500 nM of mismatched analyte (rs87C). The green dashed lines represent the respective thresholds and the black dashed lines represent the respective LODs.

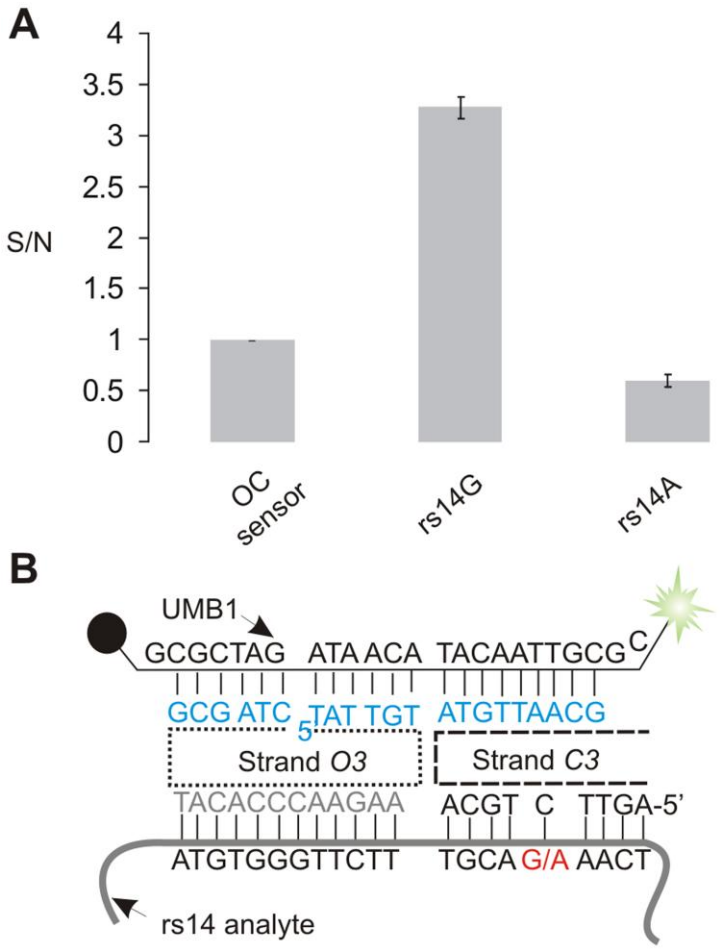

Figure 8. Design and validation of an OC sensor to selectively recognize rs1490413 SNP.

A) Signal-to-noise ratios for OC sensor designed to detect human genomic SNP rs1490413 allele G.
B) The OC sensor complex formed with UMB1 probe and rs14G analyte.

Figure 9. Design and validation of an OC sensor for recognition of secondary structure-forming fragment of *E.coli* 16S rRNA.

A) Sequences and the predicted secondary structure of stem-loop folded fragments of 16S rRNA. The nucleotide variations in *E. coli* and *B. subtilis* 16S rRNA are shown in magenta.

B) OC sensor in complex with fully matched *E.coli* f-1 sequence. MB binding arms of strands O2 and C2 are shown in cyan.

C) Signal-to-noise ratio of fluorescent response of OC sensor in the presence of absence of *E.coli* or *B. subtilis* 16S rRNA mimics. The assay was conducted in 50 mM Tris HCl, pH 7.4, 50 mM $MgCl_2$ at room temperature (22°C). The data represents the signal-to-noise ratios of three independent experiments with error bars indicating one standard deviation from the mean.

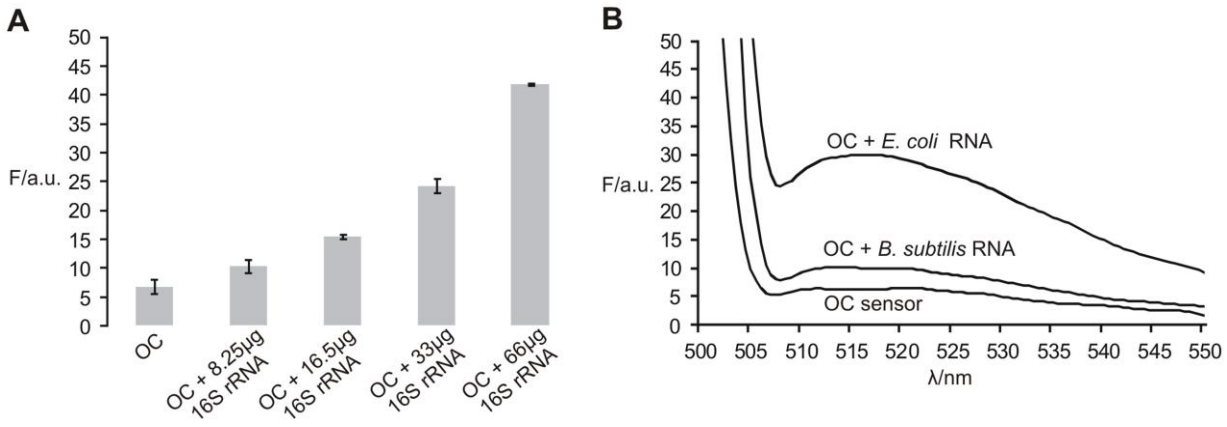

Figure 10. An OC sensor selectively recognizes bacterial 16S rRNA.

A) Fluorescent response of OC sensor in the present of various concentrations of E. coli 16S rRNA generated by *in vitro* transcription in vitro transcript. Graph depicts the mean fluorescence of three independent experiments. Error bars represent the standard deviation.

B) Fluorescent spectra of OC sensor in the presence of total RNA isolation from *E. coli* and *B. subtilis* bacteria.

CHAPTER 3: MOLECULAR LOGIC GATES FOR DNA ANALYSIS: DETECTION OF RIFAMPIN RESISTANCE IN M. TUBERCULOSIS DNA[‡]

Introduction

Molecular logic gates made of DNA have attracted significant attention because of their biocompatibility, simple design, and ability to analyze and control biological systems [48-54] To fuel further development of the field, applications of DNA-based gates to solve significant biological problems are required. Recently, our lab characterized a set of DNA logic gates (YES, NOT, AND, and OR) and demonstrated their connectivity by designing ANDNOT and XOR operations [53,54]. The gates used hybridization of DNA strands with a molecular beacon (MB) probe to produce a fluorescent output. Herein, DNA logic gates are applied to solve an important biomedical task: analysis of multiple DNA sequences containing a complex set of mutations.

Mycobacterium tuberculosis (*Mtb*) infects approximately 2 billion people all over the world and is responsible for about 2 million deaths each year [55]. Approximately 10% of all patients are infected by strains of *Mtb* that are drug-resistant; these strains are primarily resistant to antibiotics rifampin (Rif) and isoniazid [55]. Currently, there is

[‡] Work in this chapter was previously published: Cornett EM, Campbell EA, Gulenay G, et al. (2012) Molecular logic gates for DNA analysis: detection of rifampin resistance in M. tuberculosis DNA. *Angew Chem Int Ed Engl* 51:9075–9077.

an urgent need for cost-effective diagnostic methods that can detect *Mtb* in clinical samples and differentiate between drug-susceptible and drug resistant *Mtb* strains [56-60]. Several assays exist to detect mutations responsible for antibiotic resistance [56,58-62]. One of the most advanced commercial assays, Cepheid's Expert MTB/RIF [63-66], takes advantage of real-time PCR (rtPCR) and MB probes [13,67]. MB probes, first introduced by Tyagi and Kramer [12], are stem–loop-folded oligonucleotides with fluorophore and quencher dyes attached at opposite ends (Figure 11). Hybridization of an MB probe to a complementary DNA or RNA switches the probe to an elongated form, thus separating the fluorophore from the quencher. The resultant fluorescence increase can be quantitatively measured, which is the basis for the widespread application of MB probes in real-time detection of nucleic acids. In the Expert MTB/RIF assay, five MB probes were designed to span the highly variable 81-nt core of the bacterial amplicon where approximately 96% of all Rif-resistant mutations are located (Figure 11A). The probes were complementary to the drug-susceptible wild-type (WT) sequence [68]. A signal from all five MB probes indicated the presence of the WT (no mutation in the core region). Absence of a signal from all five probes indicated that a sample was *Mtb* negative. Failure of at least one MB probe to produce a signal indicated the presence of a Rif-resistant *Mtb* (Figure 1A, right). Formal logic suggests that the Expert MTB/RIF process is redundant: it uses five outputs to answer "yes" or "no" to the two following questions: 1) Is there *Mtb* DNA present in a sample? 2) Does the *Mtb* DNA contain a mutation that confers rifampin resistance? Additionally, five expensive, hard-to-optimize MB probes along with a five

channel fluorescent reader are needed for the assay. Formally, the task can be executed by using only two outputs. Herein we propose to use a DNA-based YES logic gate to answer the first question and an OR logic gate to answer the second question. Each gate uses a separate fluorescent output, thus the detection process requires only two MB probes.

Materials and Methods

Materials

All of the oligonucleotides were custom-made by Integrated DNA Technologies, Inc (Coralville, IA). Standard reagents for buffers were purchases from Fisher Scientific. DNA grade water was used for preparation of al samples and buffers. The sequences of all strands of the proposed oligonucleotide sensor as well as analytes are given in Table 2.

Fluorescence Assay

For the fluorescence assay with both YES and OR logic functions combined, all five M strands (50 nM), three F strands (200 nM), strands C, D (200 nM each), and E (100 nM), UMB1 (25 nM), and UMB2 (25 nM) were mixed in a buffer containing 50 mM $MgCl_2$, 50 mM Tris-HCl, pH 7.4, in the presence or absence of 250 nM wild-type (WT) or mutant analyte (M1–M5). Final sample volumes were 120 mL. Fluorescence spectra were recorded on a PerkinElmer (San Jose, CA) LS-55 luminescence spectrometer with a Hamamatsu xenon lamp (excitation at 550 nm; emission at 580

for UMB1 and excitation at 485 nm; emission 517 nm for UMB2) after 15 min incubation at room temperature (22°C). The data was analyzed using Microsoft Excel. The means of three independent experiments were calculated and converted to signal-to-background Figure 2. The background was considered the sample with all oligonucleotides except analyte. All signals above a threshold set at S/B=1.5 were considered true outputs for either the YES or the OR logic gates.

Results

Analyte WT represents wild-type *Mtb* sequence with no resistance-causing mutations. All five mutant sequences (named here M1–M5; see Table 2) were from the highly variable 81-nt core, each with a separate known mutation that confers Rif resistance. They were previously used for characterization of Rif resistant *Mtb* strains by conventional methods [61,62,68-71]. The YES logic gate consisted of the three DNA stands (a, b, and c in Figure 11B) and a universal MB probe (UMB1). In the presence of any Mtb DNA, either WT or Rif-resistant M1–M5, the three strands formed a complex with the target DNA and UMB1. The fluorescent complex that contained UMB1 had an arrangement of DNA strands similar to a DX tile,[7] which our lab recently studied [35]. Importantly, the DX complex was tolerant to mutations since it formed a long 36 base pair hybrid with the analyte (Figure 14). The OR gate was designed to report the presence of any of the five different drug resistance-conferring mutations across all three separate regions within the hypervariable 81-nt region of the Mtb genome. The OR gate consisted of O and C strands. Each C strand was

designed to recognize a specific mutant strain of *Mtb* that is known to cause Rif resistance. Together, the five C and the three O strands formed five fluorescent complexes with UMB2 and the five *Mtb* mutants, M1, M2, M3, M4, and M5 (Figures 12 and 13). Each fluorescent complex was formed only in the presence of the cognate mutant analyte, but not WT. Therefore, overall performance of the complete set of all O and C strands corresponded to OR logic, which produced a high fluorescent output in the presence of any *Mtb* DNA containing one of the 5 selected SNP that confer Rif-resistance, but low in the presence of WT. Pairs of O and C strands were optimized to produce high signals only in the presence of cognate mutant sequence (Figures 12 and 13). Two different O strands, M1_M4-O and M2_M3-O were utilized as uniform components for recognition of M1, M4 or M2, M3, respectively. Importantly, no signal above the background was produced by the WT Rif-susceptible sequence (Figures 12 and 13). This was achieved by designing relatively short analyte-binding arms of all M strands (7 nucleotides), which increased sensitivity for a mutation (Figure 12).

To create a functional assay, all DNA strands of both the YES and OR gates were combined with UMB1 and UMB2 in one reaction mixture and the outputs of the UMBs were measured at two different wavelengths (517 nm and 580 nm). Both the OR and YES gates functioned according to the design: the YES gate produced high output at 580 nm in the presence of both WT and the mutant sequences (Figure 15, gray bars); the OR gate generated high signal at 517 nm in the presence of any of the mutants but a low signal for the WT analyte (Figure 15, black bars). Therefore, the combination of the YES and OR gates produced a high signal at 580 nm if any *Mtb*

sequence is present, whereas a signal at 517 nm was observed only if a Rif resistant mutant sequence was present. This signal pattern can be unambiguously used for diagnostic purposes to answer the questions of the presence of an *Mtb* sequence and its Rif susceptibility.

Discussion

PCR-based *Mtb* analysis is considered to be a new method to replace time consuming culturing or error-prone sputum smear microscopy techniques [57,69]. The Expert MTB/RIF assay can detect Mtb resistance in 2 hours with high selectivity [63-65,72-74]. However, the approach is limited to interrogation of the 81- nt hypervariable fragment of the *Mtb* genome. Detection of other mutations (for example, mutations responsible for isoniazid resistance) would require introduction of additional MB probes, while current rtPCR instruments register fluorescence from only a few (5 or 6) channels. Importantly, if a sample is contaminated with the WT sequence, the assay would produce a false negative for antibiotic resistance, as all five MB probes would preferably bind the WT analyte, producing high fluorescent signal. Herein we propose the combination of YES and OR DNA logic gates to achieve accurate detection of both WT and Rif-resistant *Mtb* DNA sequences (Figure 16). The approach minimizes the number of MB probes required for both the detection of *Mtb* and Rif resistance. Therefore, a qPCR instrument with five detection channels can be replaced with a more affordable two-channel thermal cycler. Alternatively, additional OR gates can be designed to recognize other antibiotic-resistant *Mtb* strains if a multichannel qPCR

instrument is available. Thus, the study presented herein can serve as the framework for the development of a multiplex assay to determine *Mtb* presence as well as drug resistance for all major first-line antibiotics. A multiplex assay of this nature would be a valuable tool for health care providers. In either case, the presented approach is cost-efficient as the logic gates use unmodified DNA as adaptor strands, which are inexpensive synthetic oligonucleotides. Earlier, our lab reported the design of DNA logic gates that take advantage of MB probes as fluorescent reporters [27,28,32,33]. However, the constructs used expensive non-nucleotide modifications, which added to the cost of custom-made oligonucleotides. The combination of adaptor strands O and C reported herein is a new cost-efficient OR gate that demonstrates robust performance. Impressively, the 13 oligonucleotides working together in solution clearly demonstrated predictable digital response with no detectable crosstalk.

We anticipate that the use of additional strands for detection of other mutations, including those responsible for resistance to isoniazid and other antibiotics, will not compromise the performance of the assay. Indeed, the complex predesigned DNA associates of hundreds of self-assembling DNA strands can be produced at a yield of more than 90% [75,76]. Among numerous DNA logic gates reported to date, there are few applications to solve challenging practical problems. We have demonstrated that the combination of DNA logic gates can be used to perform a complex diagnostic task efficiently, affordably, and reliably. This work is a step towards employing logic gates as versatile tools for diagnosis of tuberculosis and other infectious diseases, which

opens a new application of DNA nanotechnology and DNA computation in biology and medicine.

Figures and tables

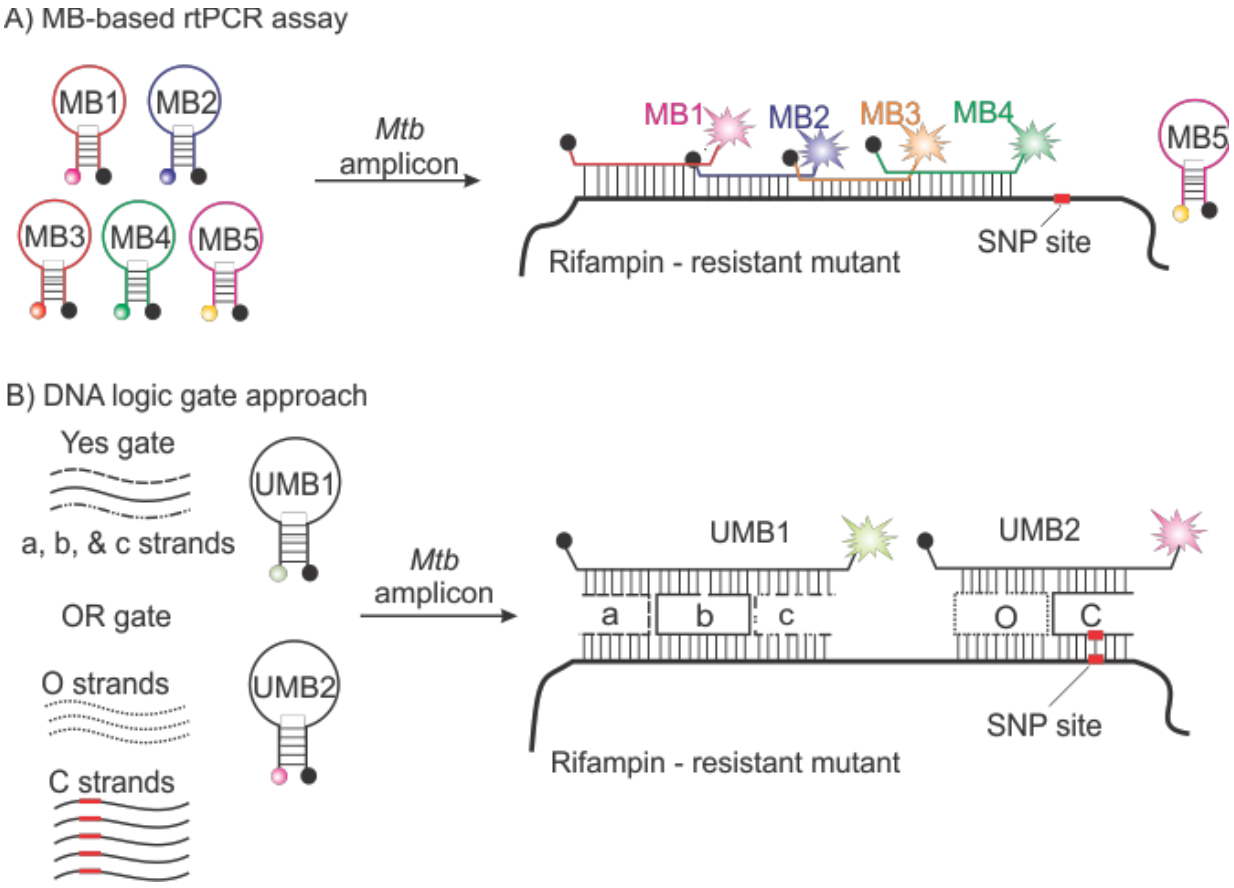

Figure 11. Molecular Beacon (MB) probe-based strategies for analysis of Rif-resistant *Mtb*.

A) Expert MTB/RIF five MB probe approach [63-65,74]. Absence of a signal from at least one MB probe (for example, MB5) indicates the presence of Rif-resistant Mtb DNA.

B) Combination of YES and OR logic gates for the detection of Mtb and its resistance to Rif. The three DNA strands (a, b, and c) form a complex with UMB1 and the analyte to report the presence of Mtb DNA. A pair of O and C strands of the OR gate forms fluorescent complex with UMB2 and the analyte only if a mutation responsible for Rif-resistance is present in the sequence. SNP = single nucleotide polymorphism.

Table 2. Sequences of oligonucleotides used in the DNA logic gate for *Mtb* DNA analysis study.

Name	Sequence	Purification
UMB 1	5‘-/TMR/CCTGGAATCATCGAACAAAGCACAGCCAG G/BHQ2/	HPLC
UMB 2	5’-/FAM/GCGTTAACATACAATAGATCGC/BHQ1/	HPLC
UMB 2’	5’-/FAM/GCGTTAACATACAATAGATCGC	SD
a	5’-TGGCTGTGCTCAGCTGGCTG G	SD
b	5’ TTCGACATGAATTGGCTTTG	SD
c	5’- GTTGTTCTGGTCTGATTCCA	SD
M1_M4-O	5‘-TATTGTGTCGGCGCTTGTGCGATC	SD
M2_M3-O	5’-TATTGTGCGGGTTGTTCTGCGATC	SD
M5-O	5‘-TATTGTGAATTGGCTCAGGCGATC	SD
M1-C	5’-GCCCACAATGTTAACG	SD
M2-C	5’-CCCAACAATGTTAACG	SD
M3-C	5‘-CCCTGCAATGTTAACG	SD
M4-C	5‘-GCCAACAATGTTAACG	SD
M5-C	5‘-GGCCCATATGTTAACG	SD
WT	5’-GCACCAGCCAGCTGAGCCAATTCATGGACCAG AACAACCCGCTGTCGGGGTTGACCCACAAGCGCC GACTGTCGGCGCTG	SD
M1	5’-GCACCAGCCAGCTGAGCCAATTCATGGACCAG AACAACCCGCTGTCGGGGTTGACCCACAAGCGCC GACTGTGGGCGCTG	SD
M2	5’-GCACCAGCCAGCTGAGCCAATTCATGGACCAG AACAACCCGCTGTTGGGGTTGACCCACAAGCGCC GACTGTCGGCGCTG	SD
M3	5’-GCACCAGCCAGCTGAGCCAATTCATGGACCAG AACAACCCGCTGCAGGGGTTGACCCACAAGCGCC GACTGTCGGCGCTG	SD
M4	5’-GCACCAGCCAGCTGAGCCAATTCATGGACCAG AACAACCCGCTGTCGGGGTTGACCCACAAGCGCC GACTGTTGGCGCTG	SD
M5	5’-GCACCAGCCAGCTGAGCCAATTCATGGGCCAG AACAACCCGCTGTCGGGGTTGACCCACAAGCGCC GACTGTCGGCGCTG	SD

* Red indicates polymorphism location.

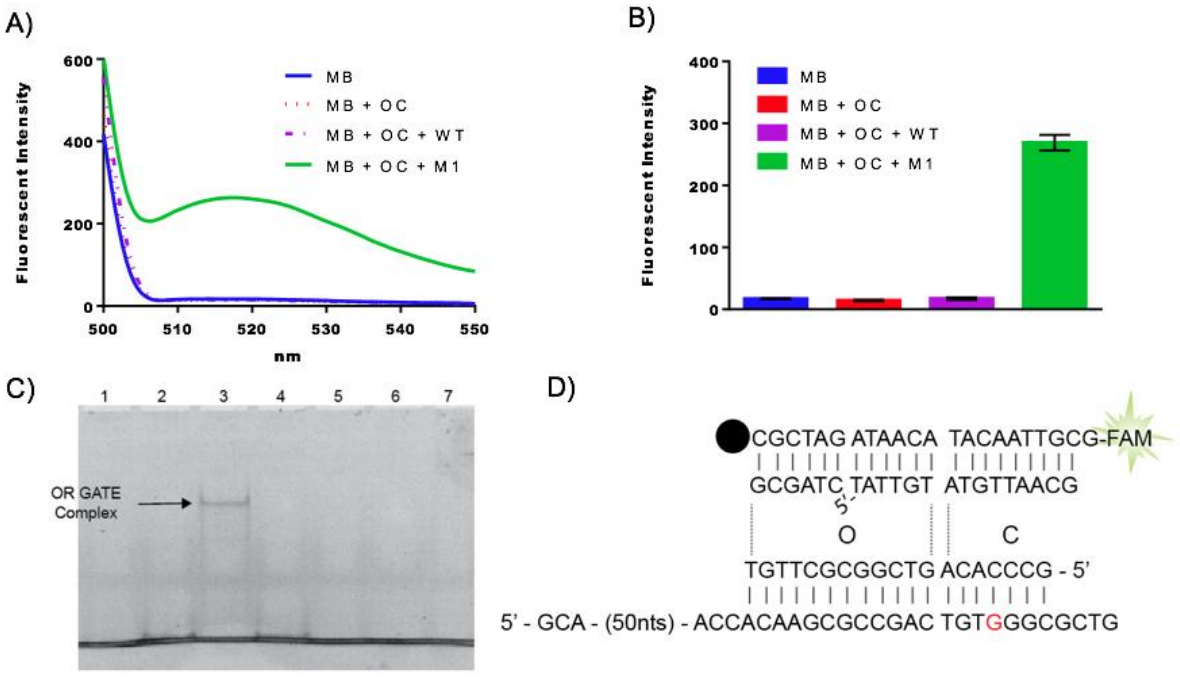

Figure 12. Design and performance of OR gate component for recognition of M1 analyte.

A) Fluorescent output and the complex formed by the OR gate component with M1 analyte. Strands M1_M4-O and M1-C (200 nM) and UMB2 (25 nM) were incubated in the absence (red) or presence of 500 nM WT (pink) or mutant M1 (green). Control sample (blue) contained only UMB2 (25 nM). Spectrum of fluorescent output between 500 and 550nm with 485nm excitation was recorded after 15 minute incubation.

B) Graph depicts the mean of three independent measurements with one standard deviation for fluorescent output at 517nm.

C) Native polyacrylamide gel electrophoresis (nPAGE) analysis of OR gate performance. Samples were mixed as described in the Materials and Methods with UMB2 replaced by UMB2' (no quencher, see table 2 for the sequence). Samples contained the following oligonucleotides: Lane 1: UMB2'; Lane 2: UMB2', M1_M2-O and M1-C; Lane 3: UMB2', M1_M4-O, M1-C and M1; Lane 4: UMB2', M1_M4-O, M1-C and WT; Lane 5: M1_M2-O; Lane 6: M1-C; Lane 7: M1. After 15 minute incubation at room temperature, 20µL of nPAGE-loading buffer (50% glycerol, 50mM Tris-HCl pH 7.4, 50mM) was added to each sample. A total of 120µL of each sample was loaded into an 8% nPAGE (1.5 mm thick) and run for 30 min at 100 V with 4℃ water circulating through a Thermo-Owl PD9S gel electrophoresis apparatus. The gel picture was taken without staining using a U:Genius gel documentation instrument. The fluorescent complex corresponding to the tetrapartite associate is indicated by the arrow.

D) Structure of fluorescent tetrapartite complex of M1_M4-O, M1-C, UMB2 and M1 analyte.

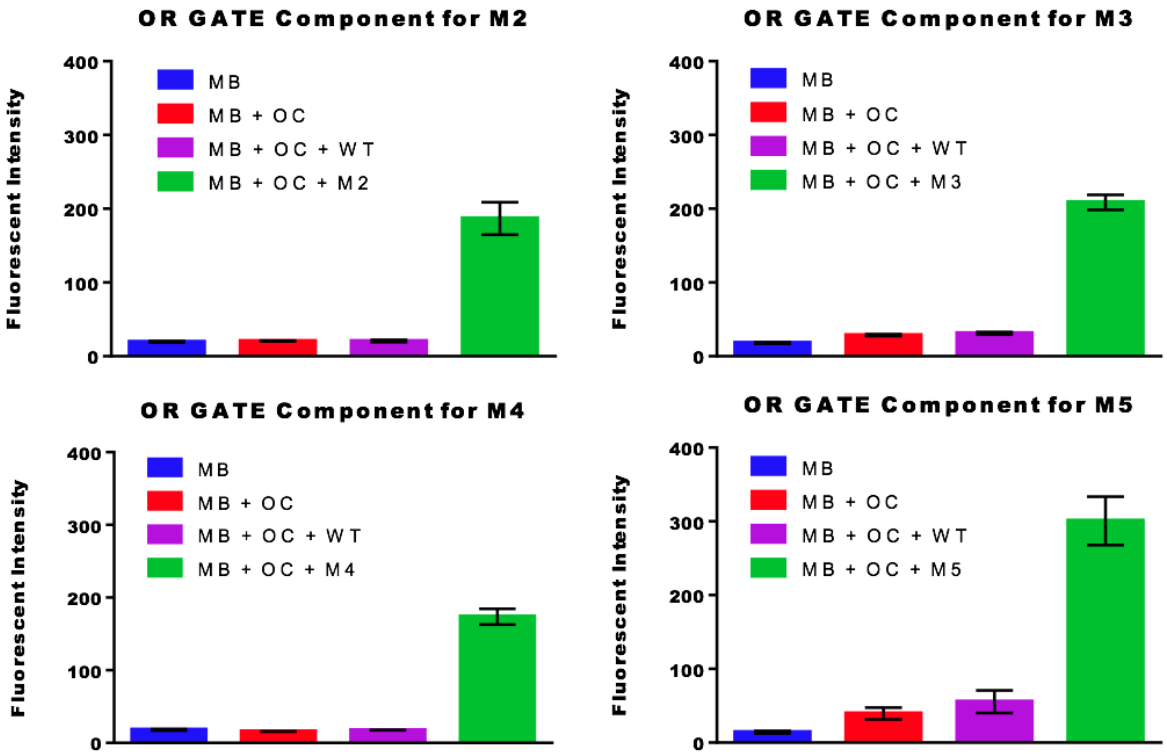

Figure 13 Fluorescent output of OR gate components for M2-M5.

Corresponding strands O (200 nM), C (100 nM) and UMB2 (25 nM) were incubated in the absence (red) or presence of WT (pink) or a mutant (green) (500 nM). Control sample (blue) contained only UMB2 (25 nM). Fluorescent output at 517 nm with 485 nm excitation was recorded after 15 min incubation. Graphs depict the mean of three independent measurements with one standard deviation.

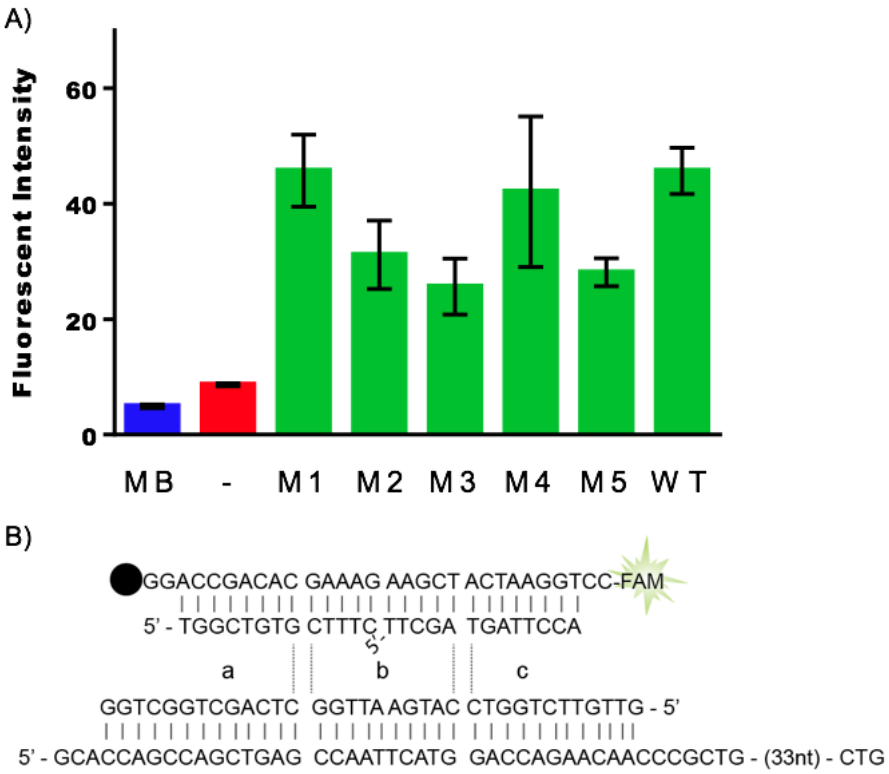

Figure 14. Design and performance of YES logic gate for recognition of *Mtb* WT DNA sequences.

A) Fluorescent output from YES gate in the presence or absence of the DNA analytes. Strands a, b (200 nM), c (100 nM) and UMB1 (25 nM) were incubated in the absence (red) or presence of mutants M1-M5 or WT analytes (500 nM). Control sample (blue) contained only UMB1 (25 nM). Fluorescent output at 580 nm with 550 nm excitation was recorded after a 15 minute incubation at room temperature. Graph depicts the mean of three independent measurements with one standard deviation.

B) Structure of fluorescent penta-partite complex containing: a, b, c, UMB1 and WT analyte.

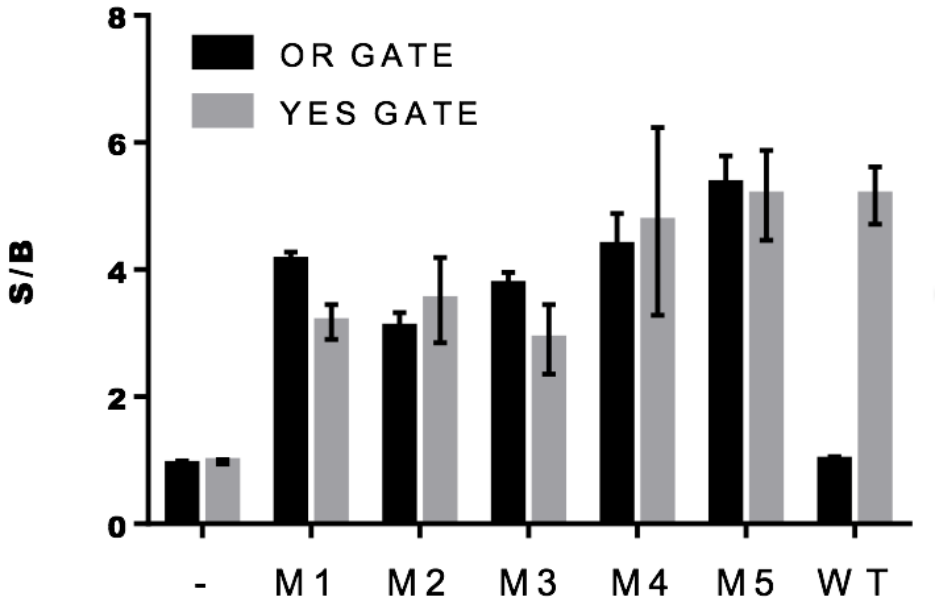

Figure 15. Combination of YES and OR gates for detection and mutation analysis of *Mtb* DNA.

All OR gate, YES gate, UMB1, and UMB2 oligonucleotides were mixed together in the absence or presence of each separate mutant or wild-type analytes. Fluorescence at 580nm for UMB1 (gray) or 517nm for UMB2 (black) was recorded after a 15 min incubation at room temperature. The graph depicts the mean signal-to-background ratio (S/B) of three independent measurements. Error bars represent the standard deviation. S/B was calculated as a ratio of fluorescence in the presence of analyte over the fluorescence in the absence of analyte.

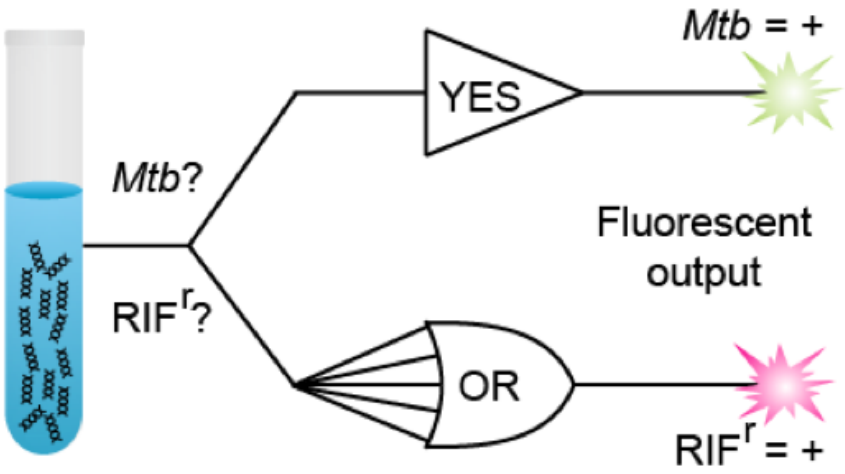

Figure 16. Graphical representation of logic gate scheme for detection and mutation analysis of *Mtb* DNA.

CHAPTER 4: BINARY REAGENTS FOR INACTIVATION OF HIV-1 REVERSE TRANSCRIPTASE

Introduction

Design and development of probes that selectively recognize and subsequently block a protein's function are important for research and drug discovery. Classical approaches have focused on optimization of inert small molecules that form non-covalent interactions with their target leading to only moderate affinity and reversible inhibition of the target's biological function. Interestingly, some of the most successful commercial drugs interact with their targets through covalent interactions, so-called "covalent inhibitors" [77-79]. Most of the covalent inhibitors currently approved for use as drugs were discovered serendipitously. Recently, concerted efforts by academia and industry have been made to rationally design and develop new covalent inhibitors [77,78]. The main impetus behind the newly minted interest in covalent inhibitors is due to the advantages they offer. These include lower dosing, uncoupling of pharmacokinetics (PK) and pharmacodynamics (PD), and decreased likelihood of resistance being formed against the inhibitor [77,80]. The limiting factor in wide-scale development of covalent inhibitors is selectively controlling the formation of the covalent bond with only a specific target. The predominant mechanism of action for covalent inhibitors is inclusion of an electrophilic moiety capable of reacting with nucleophilic amino acids on target proteins. Thus, the wide distribution of such amino acids throughout the proteome causes difficulties achieved the necessary selectivity for use as drug leads or chemical probes. Others have addressed this issue by using

bioinformatics to select targets that contain a requisite nucleophilic amino acid that is not present in similar proteins [77,81]. This ‘targeted covalent inhibitor” (TCI) approach has found success in developing covalent inhibitors for kinases. The range of proteins that can be targeted with the TCI approach is limited by the requisite of a unique nucleophilic amino acid side chain. We hypothesize that a binary approach to developing covalent inhibitors will allow a greater flexibility in designing probes to selectively recognize and inhibiting a specific target.

Design of covalent inhibitors using the binary approach.

In this application of the binary approach, two analogs of ligands (Figure 2) that bind adjacent sites of the target are conjugated to pre-reactive groups. These pre-reactive groups (Figure 2 half circles) are small molecules that fulfill three criteria. First, it is necessary that pre-reactive groups be inert toward water and biological other molecules. Second, pre-reactive groups should react with each other when in proximity and proper orientation. Finally, the reaction between pre-reactive groups should produce a new chemical group that is capable of reacting with, or modifying, amino acid side changes, protein backbone, or nucleic acid backbone (recognition event). Thus, upon binding of both ligands to the target, the pre-reactive groups will be in proximity to react and form a reactive intermediate that subsequently reacts with amino acids on the target, inhibiting its function. We recently reported a light-activated two-component covalent inhibitor designed following the binary approach that inhibits of T4 DNA polymerase. Importantly, we were able to directly compare a classical

single covalent inhibitor approach to the binary approach and found significant improvement in the selectivity of the binary inhibitor. The light-activated compounds are useful for some research applications, however, it is our goal to develop a similar inhibitor utilizing chemistry that does not require light. Such, light-free binary covalent inhibitors would be useful as chemical probes for research and potentially as drug leads. Herein, the binary approach is applied to the design of covalent inhibitors for HIV-1 reverse transcriptase (RT), an important drug target and excellent model for designing covalent inhibitors using the binary approach.

HIV-1 Reverse Transcriptase: a model target for the binary approach.

We chose HIV-1 reverse transcriptase (RT) as a model target because it is especially amenable to targeting using a binary approach, is an important drug target, and its activity is easily assayed in a variety of formats. RT is the enzyme responsible for retrotranscription of the single stranded RNA genome of HIV. To accomplish this critical task in the HIV life cycle, RT coordinates three separate enzymatic activities: RNA-dependent DNA polymerase activity, ribonuclease H acitivty, and DNA-dependent DNA polymerase activity [82,83]. RT is an asymmetric heterodimer with 66kDa and 51kDa subunits; the latter is a cleavage product of the former. RT has the characteristic DNA polymerase structure, resembling a right hand with finger, palm, and thumb substructures (Figure 17). The mechanism of RT polymerization is similar to the mechanism described for other DNA polymerase. The polymerase active site is located in the palm domain, and contains a triad of aspartic acid residues with

coordinate magnesium ions required for synthesis. A primer and template DNA or RNA bind to the finger domain, positioning the 3'-hydroxyl (3'OH) of the priming strand at the active site. Near the active site and the critical aspartate residues lies the nucleotide-binding site, where deoxynucleotide triphosphates (dNTPs) bind. Upon binding of a dNTP that forms the correct Watson-Crick base pairing with the first free base in the template strand, the confirmation of RT changes. The confirmation change positions the 3'OH of the primer in the proper position to attack the alpha phosphate of the incoming dNTP, forming a phosphodiester bond [82]. The structure and function of RT make it an excellent target for applying the binary approach. Moreover, RT is an excellent model to test new pre-reactive group chemistries.

The design of a covalent inhibitor for RT following the binary approach takes advantage of the two natural ligand binding sites located near each other: the 3' end of the primer and the nucleotide binding site (Figure 17C yellow and green). Thus, the two components of the inhibitor are analogs of the natural RT substrate: nucleotide triphosphates. We chose dTTP since previous studies have shown that modification of dTTP can be routinely accomplished and modified dTTP is still a suitable substrate for many DNA polymerases, including RT. The RT will incorporate one of the dTTP analogs and translocate down the template strand, moving the first component into the first binding site, the 3' end of the primer. Upon binding of the second component to the nucleotide binding site, the two pre-reactive groups attached to the dTTP analogs will be positioned close to each other, allowing them to react. This reaction should generate a reactive chemical that subsequently reacts with available amino acid side

chains on RT. Analysis of reported structures of RT show that two lysine residues (Lys66 and Lys65) are nearby these binding sites and may be able to react under proper conditions (Figure 17C Lys66 and Lys65).

HIV-1 RT Inhibitors

Current RT inhibitors are delineated into two classes: nucleoside reverse transcriptase inhibitors (NRTIs) and non-nucleoside reverse transcriptase inhibitors (NNRTIs) [84,85]. NRTIs are delivered as nucleosides and phosphorylated to respective nucleotide triphosphates by cellular kinases. NRTIs are known as “chain terminators” due to their mechanism of action. NRTIs are competitive inhibitors that once phosphorylated, compete with natural dNTPs for binding to the nucleotide-binding site on RT (Figure17C yellow). However, NRTIs lack a 3’OH, preventing any further elongation, thus inhibiting its polymerase activity. NNRTIs are noncompetitive inhibitors that bind at an allosteric site nearby the polymerase active site and are thought to promote a conformational shift that decreases the polymerase activities of RT. NNRTIs are highly prone to the development of resistance, but are still useful for use in patients that are treatment naïve [86]. NRTIs are also prone to the the development of resistance, but less so than NNRTIs. A major downside to NRTIs is side effects associated with NRTI inhibition of the mitochondrial DNA polymerase gamma [87,88]. However, NRTIs, the first RT inhibitors discovered, remain a critical tool in treating HIV. Thus, despite the success of current HIV treatment regimens and RT inhibitors, RT remains an important drug target that warrants further efforts to develop new inhibitors. Particularly, RT is an excellent candidate to pursue

development of covalent inhibitors, as this could directly address many of the current limitations inhibitors. Thus, we chose RT as a model target to develop binary covalent inhibitors.

Materials and Methods

Materials

All chemical were purchases from Sigma Aldrich or Fisher Scientific. The CA, SB, and TF dTTP analogs were custom synthesized in the Kolpashchikov Lab by Carlos Ledezma. All other dNTPs were from Promega or New England Biolabs. The AZT triphosphate was purchased from ChemCyte.

Gel Analysis of HIV-1 RT Elongation Products

Samples (typically 15 µL) contained 50nM of HIV-1 RT (Worthington Biochemical Corporation), 1 µM of FAM-primer(FAM-Primer: 5'/FAM/ GTC CCT GTT CGG GCG CCA) and template (5'-C TGT GTG GTC GTT CTC TTG CTA TGG GCG CCG AAC AGG GAC) in HIV RT RXN buffer (50 mM Tris pH8.3, 8 mM $MgCl_2$, 40 mM KCl). FAM-primer was purified by HPLC. For CA-TF experiments, 5µM of each CA, TF, or dTTP analog was added, as indicated, followed by incubation at 37 °C. Aliquots of each sample were removed at indicated time points (5, 10, 20 and 30 minutes) and 500µM of natural dNTPs were added. After incubation at 37 °C for an additional hour, samples were quenched by addition of an equal volume of 2X dPAGE Loading Buffer (LB) (95% Formamide, 20 mM EDTA (pH 8.0), 0.05% bromophenol blue). For SB-TF

experiments the first analog was added to a final concentration of 10 μM followed by 30 minute incubation at 37 °C. The second analog was added to a final concentration of 100 μM followed by 60 minute incubation at 37 °C. Next, 500 μM of all four natural dNTPs (dATP, dCTP, dGTP, dTTP) were added to each sample, as indicated, and incubated for 60 minutes at 37 °C. To stop the polymerase reaction, an equal volume of 2X dPAGE LB was added to each sample. Control samples to evaluate elongation by one base were quenched with dPAGE LB after the initial incubation period. For both CA and SB experiments, all samples were heated for 5 minutes prior to loading 15 μL onto a 15% 7 M urea denaturing PAGE gel that was typically run for 45 minutes (or until sufficient separation as indicated by migration of bromophenol blue) at 400 V with 55 °C water running through a Thermo Owl Electrophoresis apparatus. Gels were rinsed in deionized water and visualized using a Syngene U:Genius Gel documentation instrument which allowed detection of the fluorescently labeled FAM-primer with no additional staining.

Molecular Beacon Assay for HIV-1 RT Activity

Samples (typically 50 μL) contained 50 nM of HIV-1 RT (Worthington Biochemical Corporation), 100 nM of MB probe, and 110 nM of 12-nt Primer (sequences found in Figure18A) in HIV RT RXN buffer (50 mM Tris pH8.3, 8 mM $MgCl_2$, 40 mM KCl). CA, TF, dTTP, or AZT was added as indicated and samples were transferred into wells of a ThermoNunc 96 well flat black polystyrene micro plate. After a 5 minute incubation at 37 °C, 100 μM of dNTPs were added to each sample and

fluorescent intensity was recorded at 517 nm (485 nm excitation) using an Infinite 200 Pro plate reader. After 30 minutes, an additional aliquot of MB and 12nt primer/template mix were added to each sample and fluorescent intensity was recorded for an additional 30 minutes. Validation of the assay is shown in Figure 18B.

Molecular Dynamics Simulation

Molecular Dynamics simulations were conducted using the Protein Databank (PDB) structure 1RTD. 1RTD is a solved crystal structure of a ternary HIV-1 RT structure containing RT, primer-template, and dTTP bound to the nucleotide-binding site. Figure 19 shows the MD workflow used in this study. Each step is explained in detail below. First, the dTTP ligand analogs were drawn in Chemaxon MarvinSketch, cleaned in 3d, and exported to the PDB file format. Visual Molecular Dynamics (VMD) (http://www.ks.uiuc.edu/Research/vmd/) [89] was used to align the thymidine base of the ligand analogs with the base of the dTTP from the 1RTD structure. The newly aligned dTTP analogs were saved, and the atom information (coordinates) of the base and pre-reactive group was copied into the 1RTD PDB file followed by deletion of the original dTTP base atoms and coordinates. The original ribose and triphosphate of the dTTP in the 1RTD structure was kept in place as the best approximation of the orientation that the triphosphate group of the dTTP analogs would assume. This procedure was repeated for building structures that contained analogs translocated one position into the primer as well as in the active site. Four total structures were built (dTTP, SBdTTP, TFdTMP-SBdTTP, and SBdTMP-TFdTTP). After building the

structures, they were placed in a water box using VMD. The CHARMM force field [90,91] was used and ParamChem's CGenFF program (cgenff.paramchem.org; interface version 0.9.7.1 with force field 2b8) [90,92-94] generated the topology and parameter files for the new pre-reactive groups. As with the structure, these parameter and topology files were joined with the base and ribose from the general force field. The VMD *psfgen* plugin was used to generate a PSF file for each system. NAMD Molecular Dynamics Software (http://www.ks.uiuc.edu/Research/namd/) [95] was used to perform MD simulations on the Stokes HPC at the University of Central Florida Advanced Research Computing Center (UCF ARCC). NAMD of each strcutre was run to minimize, equilibrate water, release constraints, fully equilibrate, and finally obtain production MD data (Figure 19).

Results

Clavulanic acid (CA) and 2,3,5,6-Tetrafluoro-4-hydroxy-benzoic acid (TF) pre-reactive group pair

Initially, the natural product clavulanic acid was selected as an ideal candidate for use as a pre-reactive group. Clavulanic acid (CA) is an approved β-lactam antibiotic that inhibits bacterial β-lactamases. CA was originally discovered as a product of *Streptomyces clavuligerus* in 1976 [96], and has found widespread use in combination with other traditional β-lactam antibiotics, commonly Amoxicillin, to treat both Gram-positive and Gram-negative infections [97]. CA is a suitable candidate for use as a pre-reactive group particular due to its two-step mechanism (Figure 20). Experimental data support that upon initial binding of CA to the active site of its natural

target β-lactamase, CA acylates a serine residue causing the lactam ring to open, and yielding an imminium intermediate [96]. Tautomerization of the imminium intermediate to an enamine intermediate enables acylation of an additional serine residue, resulting in a cross-linked β-lactamase. To adapt CA for use as a pre-reactive group, we proposed to use a nucleophilic pre-reactive group pair that can function similarly to the initial β-lactamase serine residue, reacting with CA to reveal a reactive intermediate that subsequently acylates an amino acid side chain in the active site of RT. An ideal pre-reactive group pair for CA is 2,3,5,6-Tetrafluoro-4-hydroxy-benzoic acid (TF) due to its pK_a, predicted to be 6.4 for the key oxygen atom attached to the 4^{th} position of the benzylic ring. (Calculated using ChemAxon MarvinSketch). Thus, at cytosolic pH, typically above 7 [98], approximately 80% of TF would be deprotonated and could be acylated by CA if the two pre-reactive groups were in proximity. Importantly, these two pre-reactive groups were also selected since they contained carboxylic acid groups that could be used to attach these groups to dTTP through standard synthetic procedures [99-102]. The structures of CA and TF analgos of dTTP are shown in Figure 21.

The CA-TF binary reagent inhibited RT activity. CA and TF were incorporated into a primer with a template that allowed incorporation of only one TF or CA in order to simulate the use of chain terminating dideoxynucleotides (ddNTP) that would cause chain termination. Alone, both analogs had minimal effect on RT activity. However, in the presence of both analogs the RT activity was reduced significantly (Figure 22 and 23A). In an effort to confirm the covalent mechanism, we tested the effect of

incubation time on RT inactivation. The effect of a covalent inhibitor can vary in experiments with different incubation times due to the requisite time for the covalent bond to form. A challenge which disallows the use of more traditional characterization of an inhibitors effect on a target enzyme [77]. Surprisingly, incubation time had little effect on the potency of the CA-TF binary reagent, under our experimental conditions (Figure 22). In effort to further characterize the nature of the CA-TF binary reagent, we used a molecular beacon RT activity assay that allows real time monitoring (Figure18). These experiments confirmed the gel analysis, showing that CA-TF inhibited RT (Figure 22). However, TF alone also significantly inhibited RT activity, likely due to the much higher ratio of TF to primer/template in this assay compared to the gel analysis. Interestingly, after 30 minutes an additional aliquot of the primer and MB probe were added, and the sample containing both CA and TF failed to produce any increase in fluorescent signal in the subsequent 30 minutes (Figure 23A). This result suggests that the CA-TF binary reagent may indeed covalently inhibit RT. Next, to compare the CA-TF binary reagent to traditional NRTIs we used commercially available triphosphate of ziduvudine (AZT) in the same assay. In order to inhibit RT at the same level as CA-TF during the first thirty minutes of the experiment, 10X the concentration of AZT (100 μM) compared to total CA and TF was required (Figure 23B). Importantly, after the second addition of primer and MB probe, even this sample showed an increase in fluorescent intensity, indicated remaining RT activity. This was expected since AZT does not covalently inhibit RT, and this result illustrates the potential utility of a covalent mechanism of action.

Despite these promising results using the CA-TF pair, additional pre-reactive group pairs were explored due to difficulties with CA analog synthesis. Indeed, even commercial efforts to produce CA for use as an antibiotic have been plagued by the poor stability of this compound [97]. Our characterization failed to reliably determine whether the compounds used in this study contained the complete clavulanic acid ring or a decomposition product (data not shown). Fortunately, a related β-lactam compound, sulbactam, showed improved stability [103,104], but still offers a similar mechanism that is amenable to adaption for the development of a covalent inhibitor using the binary approach.

Sulbactam(SB)-TF pre-reactive group pair

Sulbactam (SB) was originally designed and synthesized as an alternative for clavulanic acid [105], and displayed lower reactivity but higher stability. Importantly, similar to CA, SB is predicted to inhibit β-lactamases through a two-step mechanism making SB an attractive option as a pre-reactive group (Figure 24) [106]. Additionally, SB also contains a carboxylic acid that was used for attachment to dTTP (Figure 21). The structure of the SB dTTP analog is shown in Figure 21. Since SB has a similar mechanism as CA, TF is an ideal pre-reactive group partner.

The SB analog of dTTP alone had little effect on RT activity at low concentrations (Figure 25). However, in the presence of both SB and TF, RT was significantly inhibited. Interestingly, the potency was greater when TF was the first analog added. Unfortunately, thorough characterization of SB analogs was plagued by

similar setbacks as CA. However, the data presented herein provides an impetus for more synthetic efforts as both SB and CA or their degradation products show promising characteristics as pre-reactive groups in a covalent inhibitor designed by following the binary approach. In order to explore the conformation of the SB and TF pre-reactive groups in the RT active site and to aid in the design of future binary inhibitors we performed molecular dynamics simulations.

Molecular dynamics (MD) of Sulbactam-TF binary reagent

MD simulations of various combinations of SB-TF binary reagent components were performed in order to sample the conformations of the pre-reactive groups in the active site of RT. Furthermore, MD simulations allowed us to sample the distances between the pre-reactive groups and RT amino acids. We also sought any evidence to explain the improved potency of TF-SB reagent when TF is incorporated into the primer. The protein database structure 1RTD [83] was used as a template to build structures for MD simulations. This structure contains the full RT heterodimer in a ternary complex with a DNA primer-template and an incoming ddTTP bound in the nucleotide-binding site (Figure 17). Thus, we built four different structures based on this template. Each structure contained different dTTP or dTTP analogs in the 3'end of the primer or in the nucleotide-binding site (Figure 17C yellow and green). As a control, we used RT in complex with dTTP bound in the nucleotide-binding site (Figure 26A). In the second structure SBdTTP was bound to the nucleotide-binding site (Figure 26B). The third structure contained SBdTMP incorporated into the primer and

TFdTTP bound to the nucleotide-binding site (Figure 26C). The fourth structure had TFdTMP incorporated into the primer and SBdTTP bound to the nucleotide-binding site (Figure 26D). All four structures were prepped in the same way, and MD production for each was collected (Table 3).

To assess the stability of each structure throughout the MD simulation, the root mean square deviation (RMSD) was calculated. RMSD measures the difference in the location of atoms throughout the trajectory. Thus, a low RMSD indicates a stable structure, as the atoms are not deviating away from there original position. RMSD values were calculated for the entire MD production trajectory in four different ways for each structure. First, the entire system compared to the initial structure prior to MD production. Second, the protein backbone compared to the initial structure prior to MD production. Third, the DNA compared to initial structure prior to MD production. Fourth, the protein backbone compared to the original 1RTD crystal structure. All four structures were remarkably stable, with average RMSD values below 3 Å (Figure 27).

To ascertain whether any favorable conformations between the pre-reactive groups and protein amino acids were formed during MD simulation, the distance between various groups throughout the trajectories were measured. Interestingly, the average distance between TF and SB in the SBdTMP-TFdTTP structure is greater than 10Å (Figure 28). However, in the TFdTMP-SBdTTP structure, that same combination which inhibited RT activity, the average distance is less than 10 Å. Furthermore, in the TFdTMP-SBdTTP structure, the TF forms a stable interaction with Lys66 due to the negative charge on the TF oxygen and positively charged lysine side

chain. This structural conformation indicates a mechanism in which TF deprotonates Lys66, which is located in a flexible loop (Figure26 green loop), allowing it to react with SB bound in the nucleotide-binding site. Over all, the MD simulations support our finding that TFdTMP-SBdTTP is more potent inhibitor of RT, due to the distances between these critical residues and offers a potential mechanism worth expiring in future studies.

Discussion

Chemical probes that covalently modify their target are extremely useful as research tools and for drug design strategies [77,107]. Using the binary approach to make covalent chemical probes offers selective control over the generation of the reactive portion of the probe. Herein, the binary approach was applied to the design of covalent inhibitors for RT, which we establish as a model for testing of future pre-reactive group pairs. The CA/SB-TF pre-reactive group pair was investigated and shows promise as an ideal candidate for future use in binary reagents. This particular reagent was explored using MD simulations to confirm possible confirmations that would allow the pre-reactive groups to react with amino acids RT. This work also creates a system to test other another important component of the binary approach that can be optimized: the linker arm between the ligand and the pre-reactive group. An allylamine linker arm was used in this study, and due to conjugation with the thymidine ring, and limited rotatable bonds, only minor conformational changes were observed during MD simulation. Future study of similar systems with more flexible

linkers may reveal more favorable confirmations between the pre-reactive groups and amino acid side chains on RT or other targets. In addition to new linker arms, efforts to create robust synthetic procedures and thorough characterization of SB and CA analogs will enable full characterization of the mechanism by which these reagents inhibit RT. CA or SB might become a general pair of reagents that can easily be conjugated to ligands for other targets to quickly generate a robust and selective chemical probe.

Figures and tables

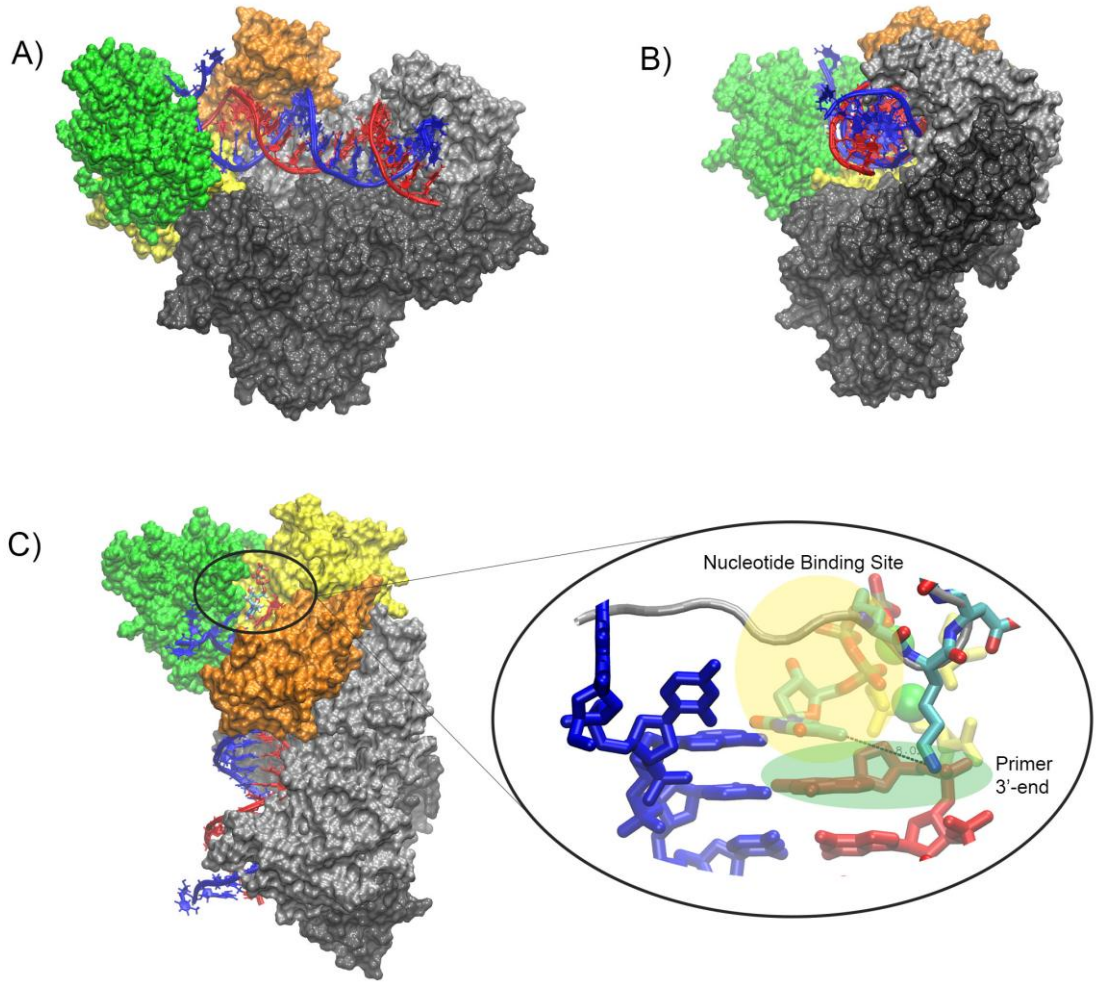

Figure 17. HIV-1 reverse transcriptase is an excellent binary approach model target.

A) Front surface rendering of HIV-1 RT [83]. Dark grey shows p51 subunit. The p66 subunit is composed of the RNaseH domain (light grey), fingers (green), palm (yellow), and thumb (orange) domains. A Primer (red) and template (blue) is bound to RT situating the 3'-end of the primer near the polymerase active site located in the palm region.
B) Side view of RT.
C) Top view of RT; insert shows close up of polymerase active site. The nucleotide binding site and primer 3'-end sites are adjacent, as required for use of the binary approach. Importantly, at least one lysine is located nearby (8 angstroms) which may react with products of binary reagents.

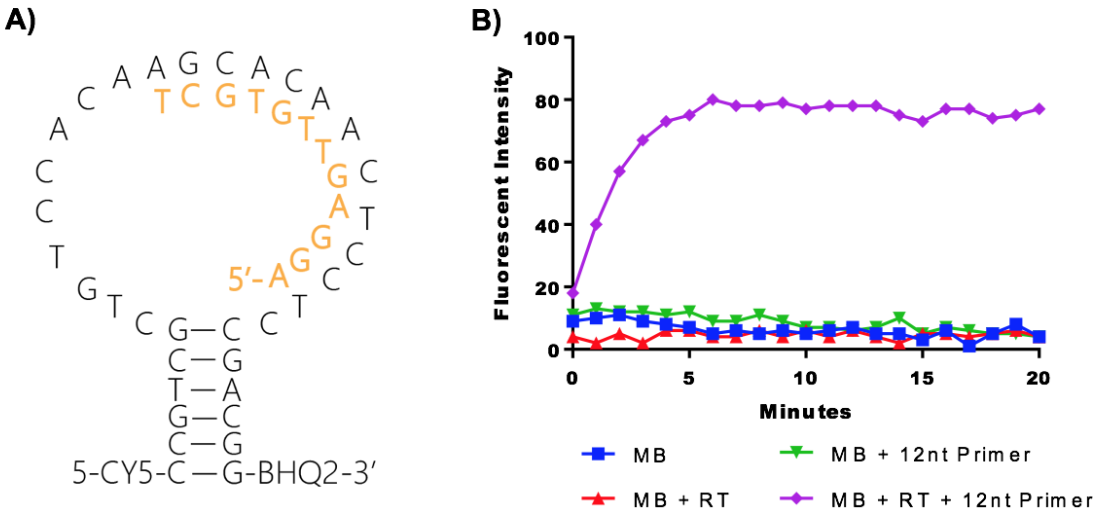

Figure 18. Molecular beacon (MB) assay for real time monitoring of HIV RT activity.

A) Sequence of MB probe (black) and primer (orange). The primer was designed so the 3' end would be adjacent to an adenine in the template to ensure that a dTTP analog would be encorporated.
B) Fluorescent intensity of MB probe in the absence or presence of RT and primer.

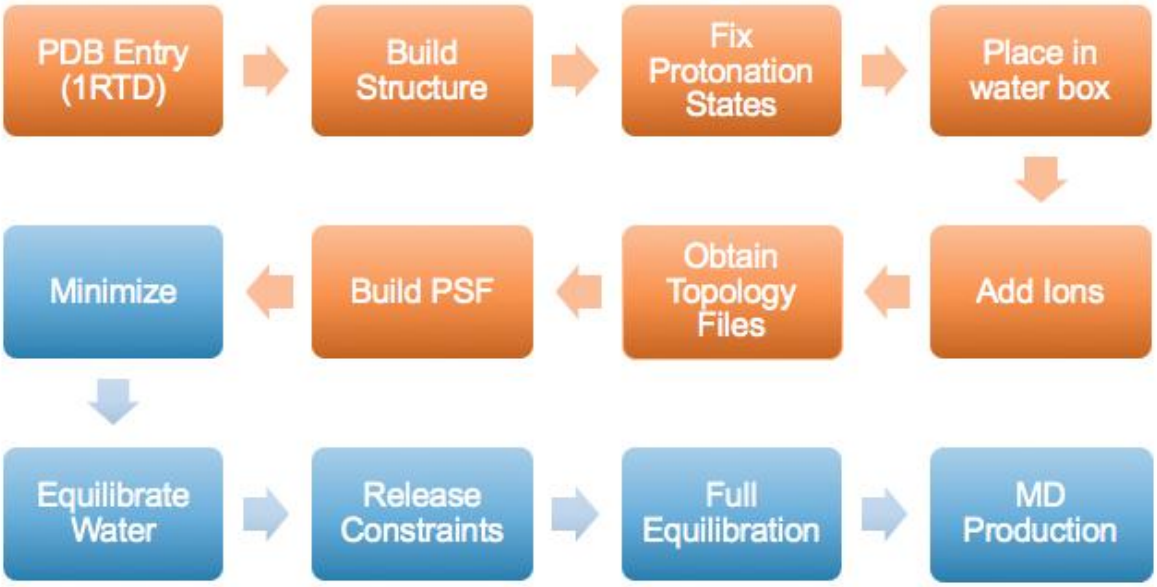

Figure 19. Molecular Dynamics (MD) workflow.

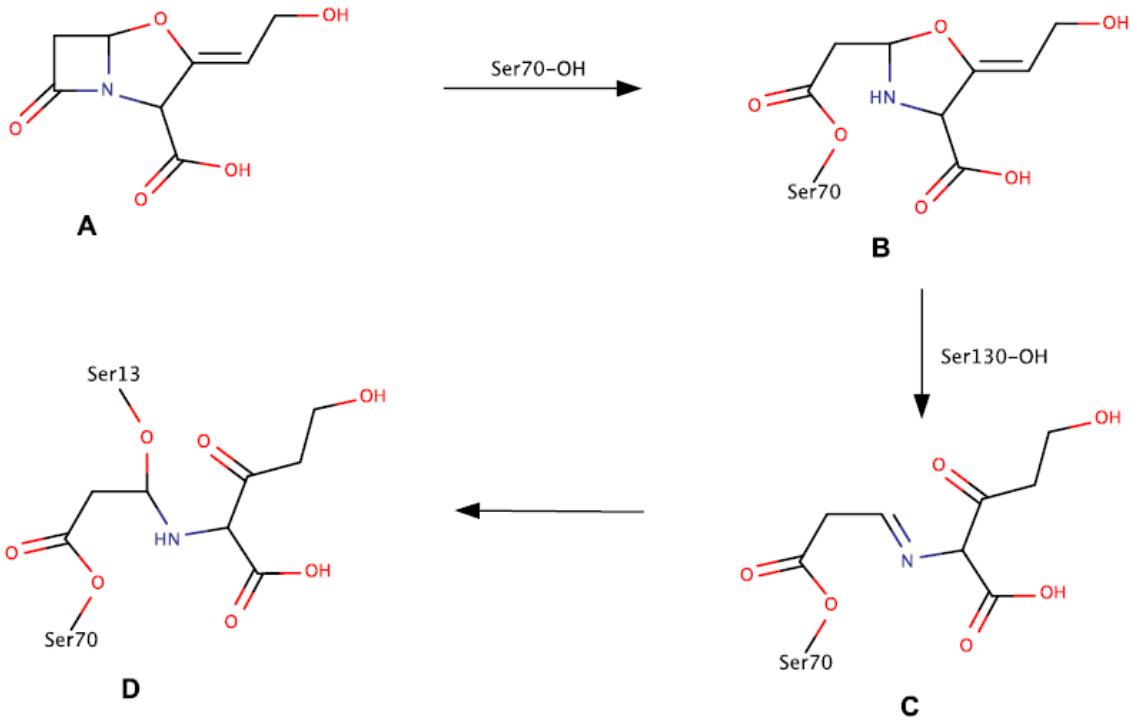

Figure 20. Mechanism for clavulanic acid inhibition of β-lactamase.

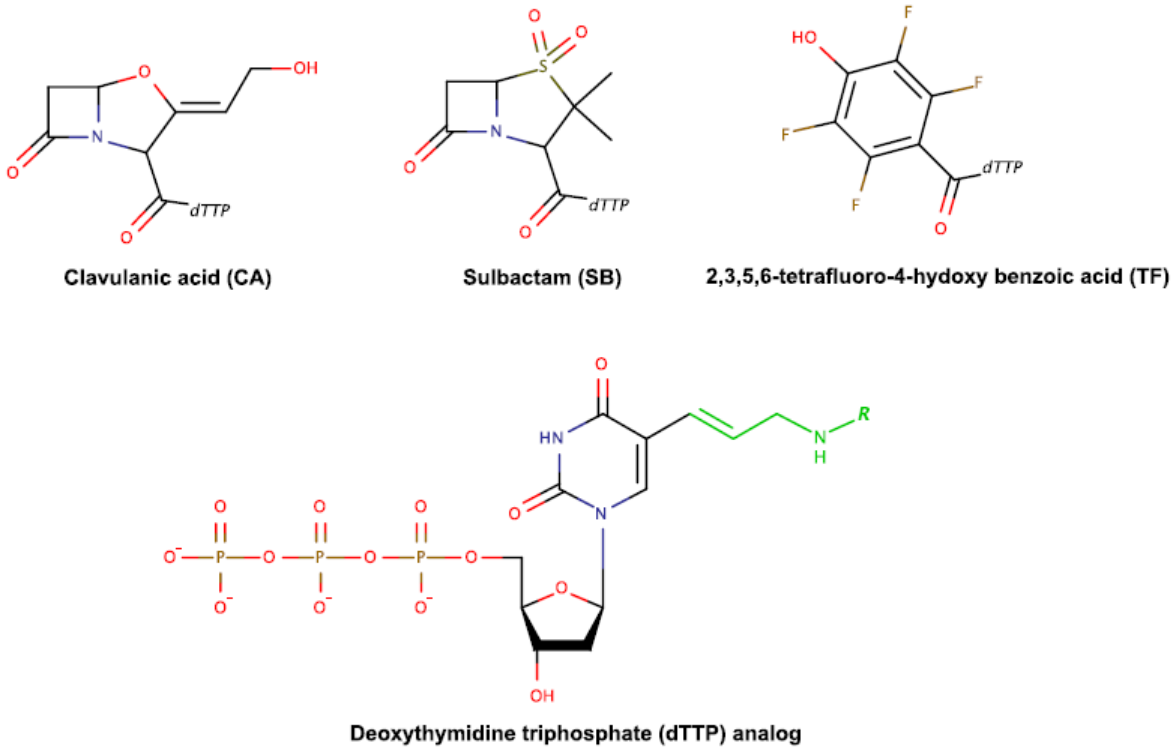

Figure 21. CA, SB, and TF dTTP analog structures.

Clavulanic acid (CA), sulbactam (SB), and 2,3,5,6-tetrafluoro-4-hydroxy benzoic acid (TF) analogs of dTTP were synthesized by acylating the amine group of the allyamine linker with N-hydroxysuccinimide esters of each pre-reactive group, as previously described [99,101,102]. Green in dTTP structure indicates allylamine linker arm.

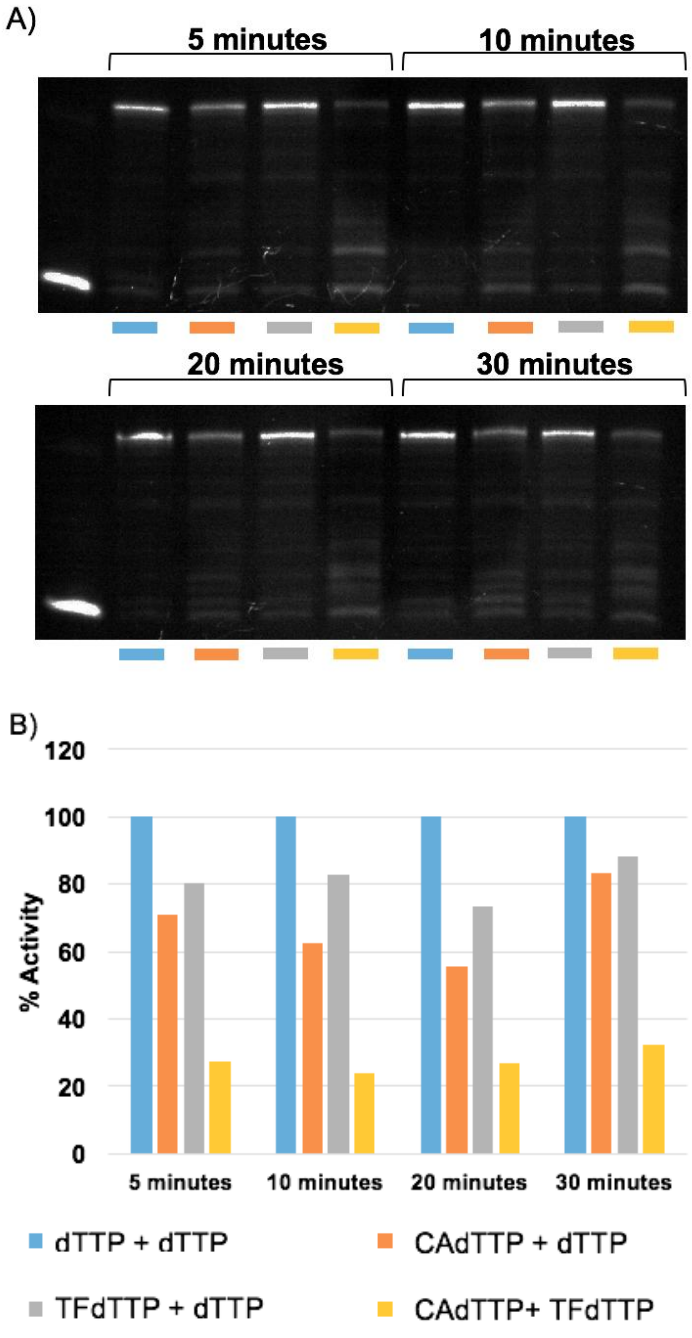

Figure 22. CA-TF Binary Reagent Inhibits RT.

A) Gel analysis of RT activity. Samples contents are indicated by color in part B.
B) Quantification of the gel bands from A.

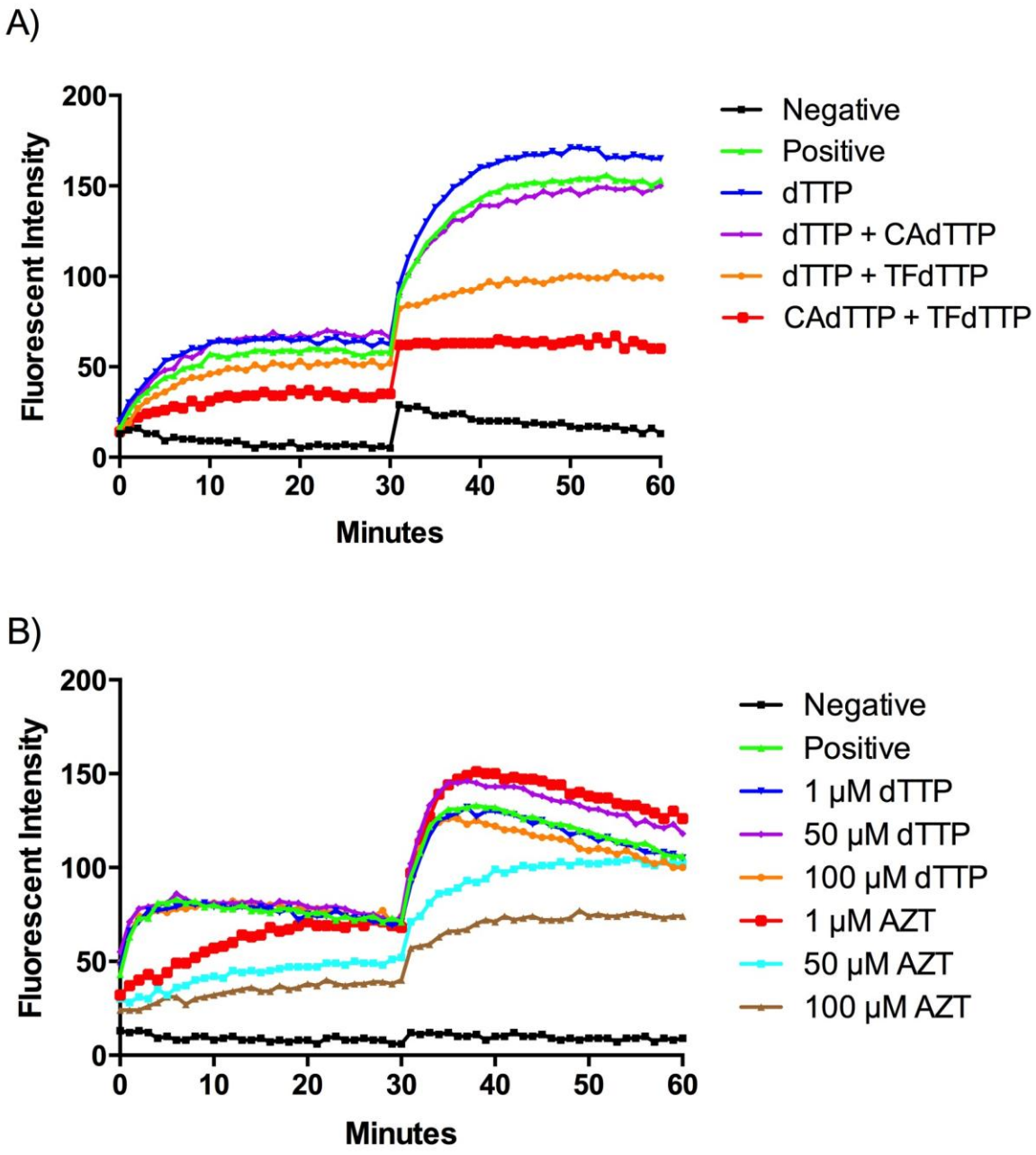

Figure 23. Comparison between binary reagent CA-TF and NRTI AZT.

A) CA-TF covalent inhibitor inactivates RT. During the first 30 minute incubation the CA-TF reagent inhibits RT activity aproximatley 50%. However, after addition of another aliquot of MB and primer at 30 minutes, the RT shows no activity in the CA-TF sample, indicating inactivation

B) AZT inhibits RT, yet even at concentration 10X higher than used for the CA-TF binary reagent, RT retains residual activity during the entire 60 minute experiment.

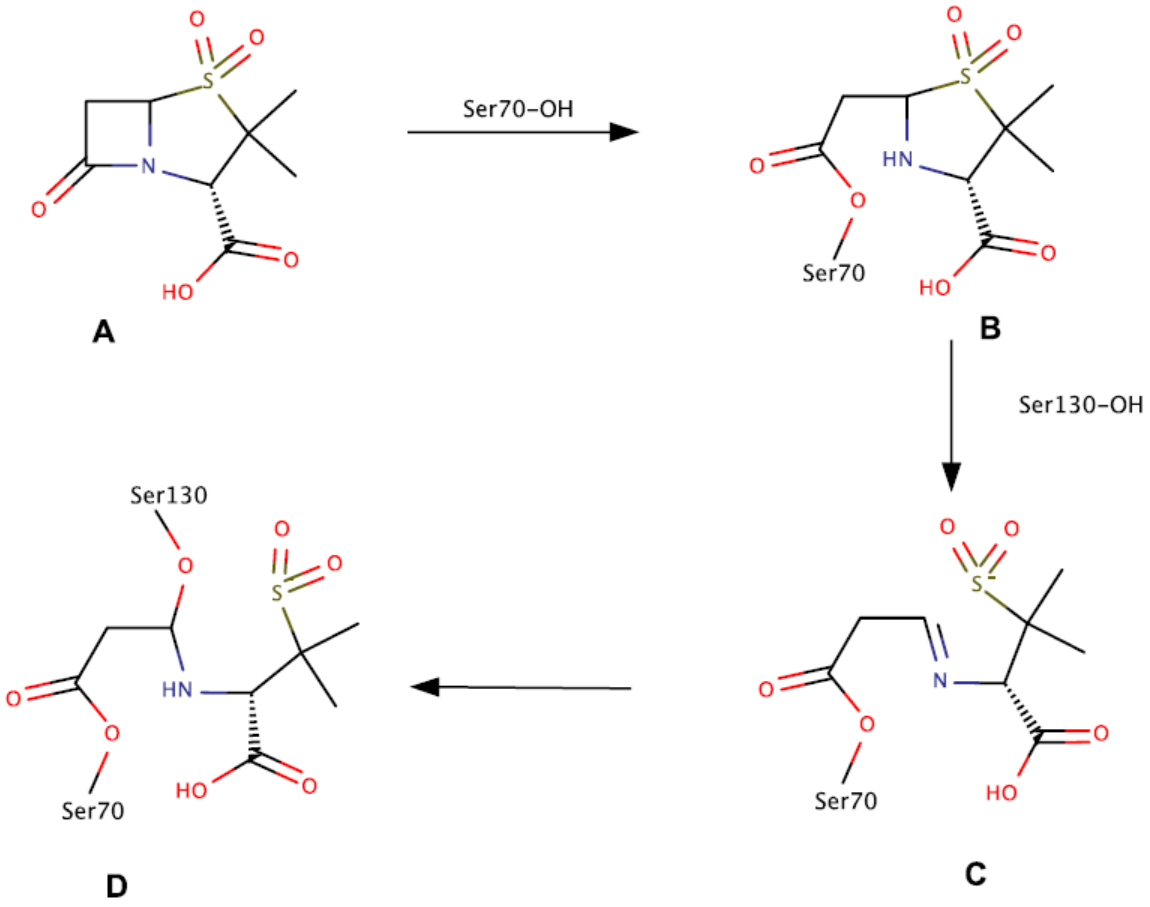

Figure 24. Mechanism of sulbactam inhibition of β-lactamase.

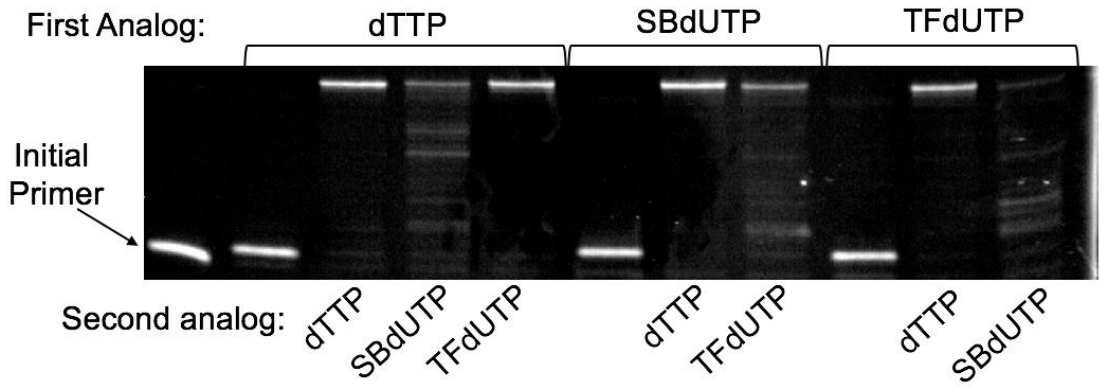

Figure 25. SB-TF binary reagent inhibits RT.

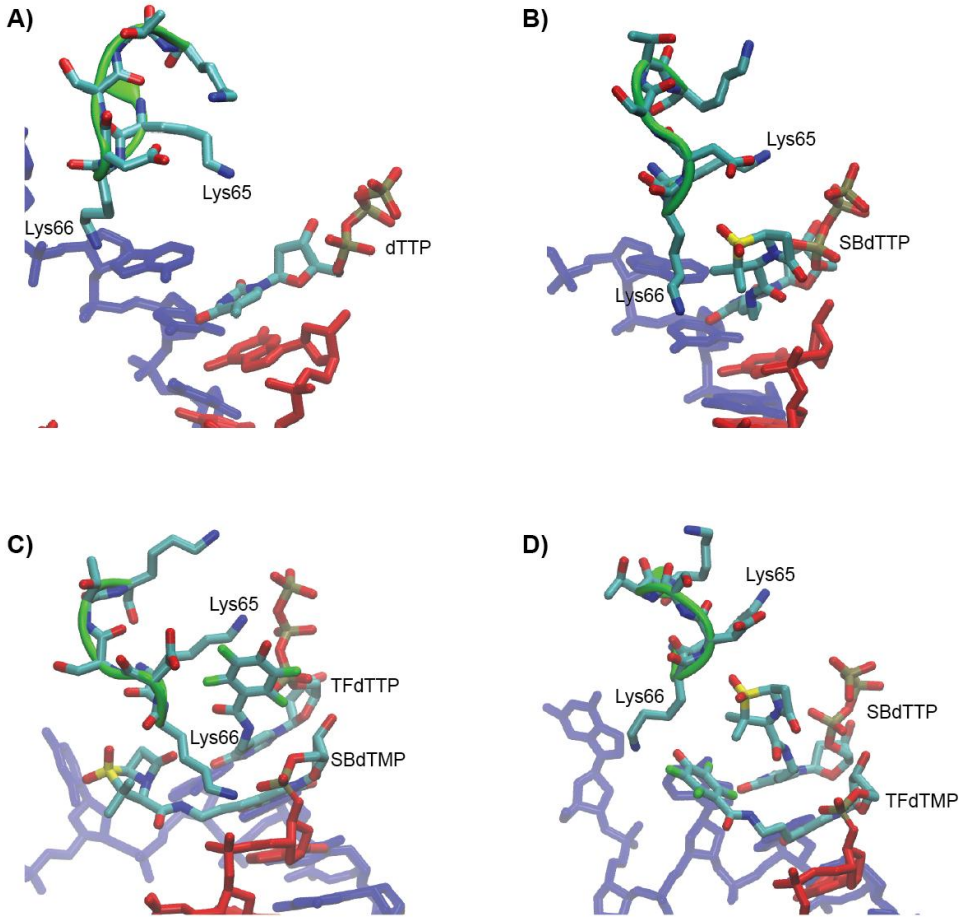

Figure 26. Active sites of RT structures used in MD study.

A) dTTP: RT structure with dTTP bound to the nucleotide binding site.
B) SBdTTP. RT structure with dTTP bound to the nucleotide binding site.
C) SBdTMP_TFdTTP: RT structure with SBdTMP at the 3'end of the primer and TFdTTP bound to the nucleotide binding site.
D) TFdTMP_SBdTTP RT structure with TFdTMP at the 3'end of the primer and SBdTTP bound to the nucleotide binding site.

Table 3. RT structures and production time from Molecular Dyanmics Simulations

RT Structure	Production Time
dTTP	8.8 ns
SBdTTP	14.6 ns
SBdTMP_TFdTTP	12.5 ns
TFdTMP_SBdTTP	12.5 ns

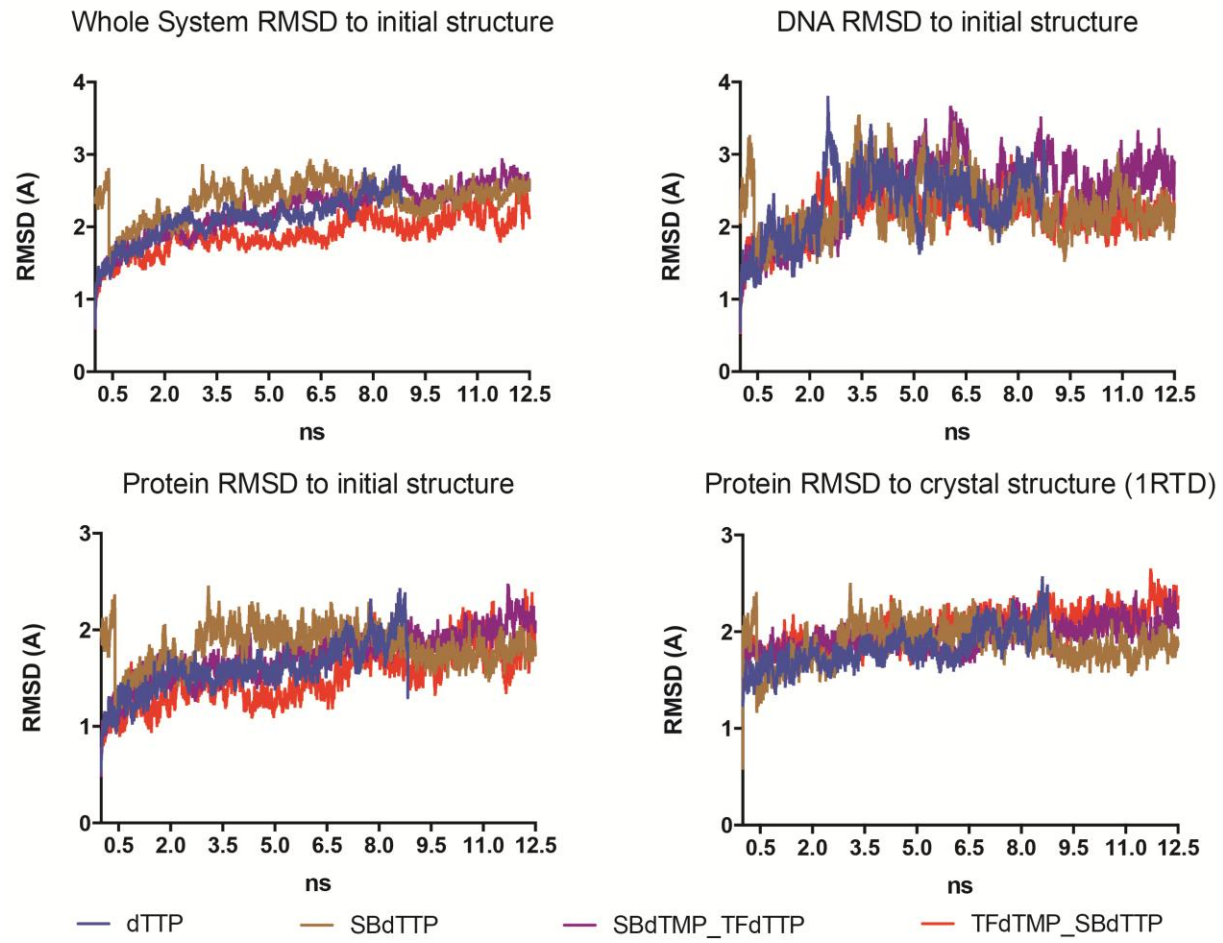

Figure 27. RMSD values for MD simulations.

The protein backbone or DNA (top right only) of all structures was aligned and RMSD values were calculated using VMD RMSD trajectory tool by comparing each frame of MD simulation trajectory data to either the initial structure prior to production or to the original crystal structure from the protein database (1RTD). These RMSD indicate all structures were stable under the force field used in MD simulation.

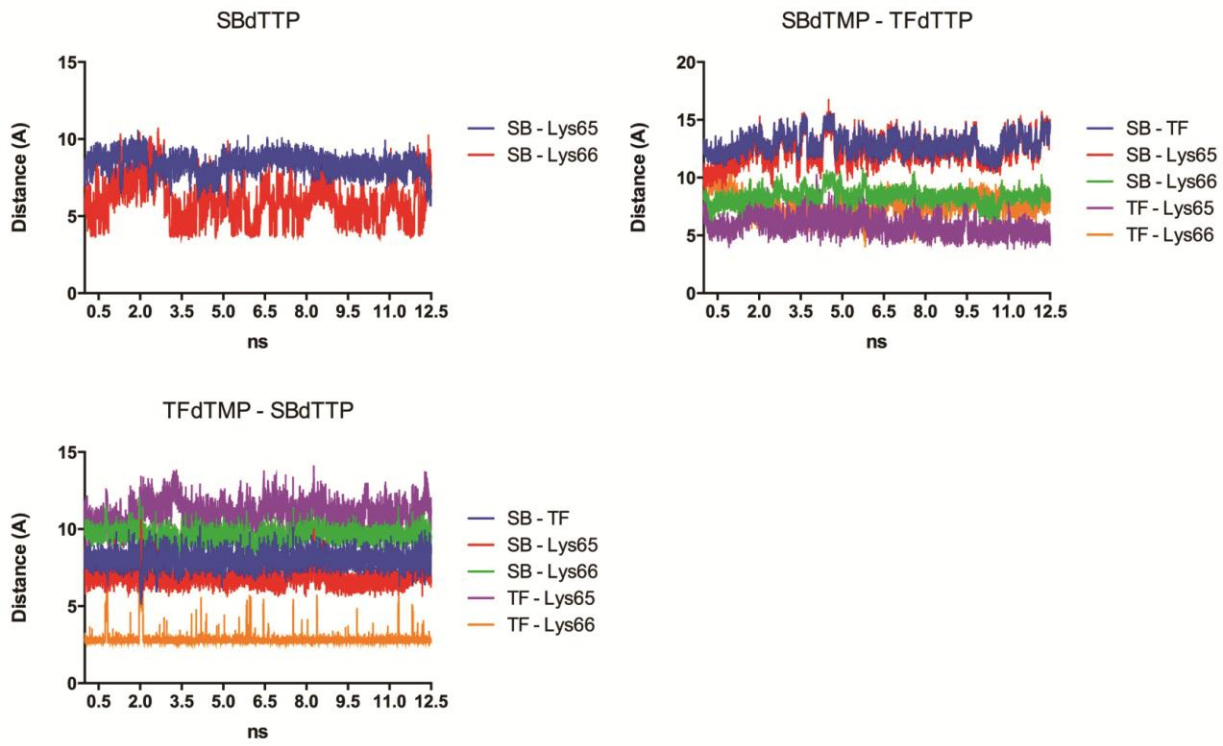

Figure 28. Distance between pre-reactive groups and RT lysine residues.

In three of the MD structures, the distance between pre-reactive groups and RT lysine residues were calculated through the entire trajectory. Measurements of SB were from the carbonyl carbon in the β-lactam ring. TF was measured from the terminal oxygen. Lysine residues were measured from the nitrogen in the lysine side chain.

APPENDIX: COPYRIGHT PERMISSION

JOHN WILEY AND SONS LICENSE TERMS AND CONDITIONS

Mar 12, 2015

This Agreement between Evan M Cornett ("You") and John Wiley and Sons ("John Wiley and Sons") consists of your order details and the terms and conditions provided by John Wiley and Sons and Copyright Clearance Center.

License Number	3565990121012
License date	Feb 11, 2015
Licensed Content Publisher	John Wiley and Sons
Licensed Content Publication	Angewandte Chemie
Licensed Content Title	Molecular Logic Gates for DNA Analysis: Detection of Rifampin Resistance in M. tuberculosis DNA
Licensed Content Author	Evan M. Cornett,Eleanor A. Campbell,George Gulenay,Evan Peterson,Neha Bhaskar,Dmitry M. Kolpashchikov
Licensed Content Date	Aug 7, 2012
Pages	3
Type of use	Dissertation/Thesis
Requestor type	Author of this Wiley article
Format	Print and electronic
Portion	Full article
Will you be translating?	No
Title of your thesis / dissertation	A BINARY APPORACH FOR SELECTIVE RECOGNITION OF NUCLEIC ACIDS AND PROTEINS
Expected completion date	May 2015
Expected size (number of pages)	80
Requestor Location	Evan M Cornett 606 Grenadine Court None None WINTER PARK, FL 32792 United States Attn: Evan M Cornett
Billing Type	Invoice
Billing Address	Evan M Cornett 606 Grenadine Court None None WINTER PARK, FL 32792 United States Attn: Evan M Cornett
Total	**0.00 USD**

Terms and Conditions

TERMS AND CONDITIONS

This copyrighted material is owned by or exclusively licensed to John Wiley & Sons, Inc. or one of its group companies (each

a"Wiley Company") or handled on behalf of a society with which a Wiley Company has exclusive publishing rights in relation to a particular work (collectively "WILEY"). By clicking ‘accept’ in connection with completing this licensing transaction, you agree that the following terms and conditions apply to this transaction (along with the billing and payment terms and conditions established by the Copyright Clearance Center Inc., ("CCC's Billing and Payment terms and conditions"), at the time that you opened your Rightslink account (these are available at any time at http://myaccount.copyright.com).

Terms and Conditions

- The materials you have requested permission to reproduce or reuse (the "Wiley Materials") are protected by copyright.
- You are hereby granted a personal, non-exclusive, non-sub licensable (on a stand-alone basis), non-transferable, worldwide, limited license to reproduce the Wiley Materials for the purpose specified in the licensing process. This license is for a one-time use only and limited to any maximum distribution number specified in the license. The first instance of republication or reuse granted by this licence must be completed within two years of the date of the grant of this licence (although copies prepared before the end date may be distributed thereafter). The Wiley Materials shall not be used in any other manner or for any other purpose, beyond what is granted in the license. Permission is granted subject to an appropriate acknowledgement given to the author, title of the material/book/journal and the publisher. You shall also duplicate the copyright notice that appears in the Wiley publication in your use of the Wiley Material. Permission is also granted on the understanding that nowhere in the text is a previously published source acknowledged for all or part of this Wiley Material. Any third party content is expressly excluded from this permission.
- With respect to the Wiley Materials, all rights are reserved. Except as expressly granted by the terms of the license, no part of the Wiley Materials may be copied, modified, adapted (except for minor reformatting required by the new Publication), translated, reproduced, transferred or distributed, in any form or by any means, and no derivative works may be made based on the Wiley Materials without the prior permission of the respective copyright owner. You may not alter, remove or suppress in any manner any copyright, trademark or other notices displayed by the Wiley Materials. You may not license, rent, sell, loan, lease, pledge, offer as security, transfer or assign the Wiley Materials on a stand-alone basis, or any of the rights granted to you hereunder to any other person.
- The Wiley Materials and all of the intellectual property rights therein shall at all times remain the exclusive property of John Wiley & Sons Inc, the Wiley Companies, or their respective licensors, and your interest therein is only that of having possession of and the right to reproduce the Wiley Materials pursuant to Section 2 herein during the continuance of this Agreement. You agree that you own no right, title or interest in or to the Wiley Materials or any of the intellectual property rights therein. You shall have no rights hereunder other than the license as provided for above in Section 2. No right, license or interest to any trademark, trade name, service mark or other branding ("Marks") of WILEY or its licensors is granted hereunder, and you agree that you shall not assert any such right, license or interest with respect thereto.
- NEITHER WILEY NOR ITS LICENSORS MAKES ANY WARRANTY OR REPRESENTATION OF ANY KIND TO YOU OR ANY THIRD PARTY, EXPRESS, IMPLIED OR STATUTORY, WITH RESPECT TO THE MATERIALS OR THE ACCURACY OF ANY INFORMATION CONTAINED IN THE MATERIALS, INCLUDING, WITHOUT LIMITATION, ANY IMPLIED WARRANTY OF MERCHANTABILITY, ACCURACY, SATISFACTORY QUALITY, FITNESS FOR A PARTICULAR PURPOSE, USABILITY, INTEGRATION OR NON-INFRINGEMENT AND ALL SUCH WARRANTIES ARE HEREBY EXCLUDED BY WILEY AND ITS LICENSORS AND WAIVED BY YOU
- WILEY shall have the right to terminate this Agreement immediately upon breach of this Agreement by you.
- You shall indemnify, defend and hold harmless WILEY, its Licensors and their respective directors, officers, agents and employees, from and against any actual or threatened claims, demands, causes of action or proceedings arising from any breach of this Agreement by you.
- IN NO EVENT SHALL WILEY OR ITS LICENSORS BE LIABLE TO YOU OR ANY OTHER PARTY OR ANY OTHER PERSON OR ENTITY FOR ANY SPECIAL, CONSEQUENTIAL, INCIDENTAL, INDIRECT, EXEMPLARY OR PUNITIVE DAMAGES, HOWEVER CAUSED, ARISING OUT OF OR IN CONNECTION WITH THE DOWNLOADING, PROVISIONING, VIEWING OR USE OF THE MATERIALS REGARDLESS OF THE FORM OF ACTION, WHETHER

FOR BREACH OF CONTRACT, BREACH OF WARRANTY, TORT, NEGLIGENCE, INFRINGEMENT OR OTHERWISE (INCLUDING, WITHOUT LIMITATION, DAMAGES BASED ON LOSS OF PROFITS, DATA, FILES, USE, BUSINESS OPPORTUNITY OR CLAIMS OF THIRD PARTIES), AND WHETHER OR NOT THE PARTY HAS BEEN ADVISED OF THE POSSIBILITY OF SUCH DAMAGES. THIS LIMITATION SHALL APPLY NOTWITHSTANDING ANY FAILURE OF ESSENTIAL PURPOSE OF ANY LIMITED REMEDY PROVIDED HEREIN.

- Should any provision of this Agreement be held by a court of competent jurisdiction to be illegal, invalid, or unenforceable, that provision shall be deemed amended to achieve as nearly as possible the same economic effect as the original provision, and the legality, validity and enforceability of the remaining provisions of this Agreement shall not be affected or impaired thereby.

- The failure of either party to enforce any term or condition of this Agreement shall not constitute a waiver of either party's right to enforce each and every term and condition of this Agreement. No breach under this agreement shall be deemed waived or excused by either party unless such waiver or consent is in writing signed by the party granting such waiver or consent. The waiver by or consent of a party to a breach of any provision of this Agreement shall not operate or be construed as a waiver of or consent to any other or subsequent breach by such other party.

- This Agreement may not be assigned (including by operation of law or otherwise) by you without WILEY's prior written consent.

- Any fee required for this permission shall be non-refundable after thirty (30) days from receipt by the CCC.

- These terms and conditions together with CCC's Billing and Payment terms and conditions (which are incorporated herein) form the entire agreement between you and WILEY concerning this licensing transaction and (in the absence of fraud) supersedes all prior agreements and representations of the parties, oral or written. This Agreement may not be amended except in writing signed by both parties. This Agreement shall be binding upon and inure to the benefit of the parties' successors, legal representatives, and authorized assigns.

- In the event of any conflict between your obligations established by these terms and conditions and those established by CCC's Billing and Payment terms and conditions, these terms and conditions shall prevail.

- WILEY expressly reserves all rights not specifically granted in the combination of (i) the license details provided by you and accepted in the course of this licensing transaction, (ii) these terms and conditions and (iii) CCC's Billing and Payment terms and conditions.

- This Agreement will be void if the Type of Use, Format, Circulation, or Requestor Type was misrepresented during the licensing process.

- This Agreement shall be governed by and construed in accordance with the laws of the State of New York, USA, without regards to such state's conflict of law rules. Any legal action, suit or proceeding arising out of or relating to these Terms and Conditions or the breach thereof shall be instituted in a court of competent jurisdiction in New York County in the State of New York in the United States of America and each party hereby consents and submits to the personal jurisdiction of such court, waives any objection to venue in such court and consents to service of process by registered or certified mail, return receipt requested, at the last known address of such party.

WILEY OPEN ACCESS TERMS AND CONDITIONS

Wiley Publishes Open Access Articles in fully Open Access Journals and in Subscription journals offering Online Open. Although most of the fully Open Access journals publish open access articles under the terms of the Creative Commons Attribution (CC BY) License only, the subscription journals and a few of the Open Access Journals offer a choice of Creative Commons Licenses:: Creative Commons Attribution (CC-BY) license Creative Commons Attribution Non-Commercial (CC-BY-NC) license and Creative Commons Attribution Non-Commercial-NoDerivs (CC-BY-NC-ND) License. The license type is clearly identified on the article.

Copyright in any research article in a journal published as Open Access under a Creative Commons License is retained by the author(s). Authors grant Wiley a license to publish the article and identify itself as the original publisher. Authors also grant any third party the right to use the article freely as long as its integrity is maintained and its original authors, citation details and publisher are identified as follows: [Title of Article/Author/Journal Title and Volume/Issue. Copyright (c) [year] [copyright owner as specified in the Journal]. Links to the final article on Wiley's website are encouraged where applicable.

The Creative Commons Attribution License

The Creative Commons Attribution License (CC-BY) allows users to copy, distribute and transmit an article, adapt the article and make commercial use of the article. The CC-BY license permits commercial and non-commercial re-use of an open access article, as long as the author is properly attributed.

The Creative Commons Attribution License does not affect the moral rights of authors, including without limitation the right not to have their work subjected to derogatory treatment. It also does not affect any other rights held by authors or third parties in the article, including without limitation the rights of privacy and publicity. Use of the article must not assert or imply, whether implicitly or explicitly, any connection with, endorsement or sponsorship of such use by the author, publisher or any other party associated with the article.

For any reuse or distribution, users must include the copyright notice and make clear to others that the article is made available under a Creative Commons Attribution license, linking to the relevant Creative Commons web page.

To the fullest extent permitted by applicable law, the article is made available as is and without representation or warranties of any kind whether express, implied, statutory or otherwise and including, without limitation, warranties of title, merchantability, fitness for a particular purpose, non-infringement, absence of defects, accuracy, or the presence or absence of errors.

Creative Commons Attribution Non-Commercial License

The Creative Commons Attribution Non-Commercial (CC-BY-NC) License permits use, distribution and reproduction in any medium, provided the original work is properly cited and is not used for commercial purposes.(see below)

Creative Commons Attribution-Non-Commercial-NoDerivs License

The Creative Commons Attribution Non-Commercial-NoDerivs License (CC-BY-NC-ND) permits use, distribution and reproduction in any medium, provided the original work is properly cited, is not used for commercial purposes and no modifications or adaptations are made. (see below)

Use by non-commercial users

For non-commercial and non-promotional purposes, individual users may access, download, copy, display and redistribute to colleagues Wiley Open Access articles, as well as adapt, translate, text- and data-mine the content subject to the following conditions:

- The authors' moral rights are not compromised. These rights include the right of "paternity" (also known as "attribution" - the right for the author to be identified as such) and "integrity" (the right for the author not to have the work altered in such a way that the author's reputation or integrity may be impugned).
- Where content in the article is identified as belonging to a third party, it is the obligation of the user to ensure that any reuse complies with the copyright policies of the owner of that content.
- If article content is copied, downloaded or otherwise reused for non-commercial research and education purposes, a link to the appropriate bibliographic citation (authors, journal, article title, volume, issue, page numbers, DOI and the link to the definitive published version on **Wiley Online Library**) should be maintained. Copyright notices and disclaimers must not be deleted.
- Any translations, for which a prior translation agreement with Wiley has not been agreed, must prominently display the statement: "This is an unofficial translation of an article that appeared in a Wiley publication. The publisher has not endorsed this translation."

Use by commercial "for-profit" organisations

Use of Wiley Open Access articles for commercial, promotional, or marketing purposes requires further explicit permission from Wiley and will be subject to a fee. Commercial purposes include:

- Copying or downloading of articles, or linking to such articles for further redistribution, sale or licensing;
- Copying, downloading or posting by a site or service that incorporates advertising with such content;

- The inclusion or incorporation of article content in other works or services (other than normal quotations with an appropriate citation) that is then available for sale or licensing, for a fee (for example, a compilation produced for marketing purposes, inclusion in a sales pack)
- Use of article content (other than normal quotations with appropriate citation) by for-profit organisations for promotional purposes
- Linking to article content in e-mails redistributed for promotional, marketing or educational purposes;
- Use for the purposes of monetary reward by means of sale, resale, licence, loan, transfer or other form of commercial exploitation such as marketing products
- Print reprints of Wiley Open Access articles can be purchased from: corporatesales@wiley.com

Further details can be found on Wiley Online Library http://olabout.wiley.com/WileyCDA/Section/id-410895.html

Other Terms and Conditions:

v1.9

Questions? customercare@copyright.com or +1-855-239-3415 (toll free in the US) or +1-978-646-2777.

Gratis licenses (referencing $0 in the Total field) are free. Please retain this printable license for your reference. No payment is required.

REFERENCES

[1] F.K. Winkler, D.W. Banner, C. Oefner, D. Tsernoglou, R.S. Brown, S.P. Heathman, et al., The crystal structure of EcoRV endonuclease and of its complexes with cognate and non-cognate DNA fragments, Embo J. 12 (1993) 1781–1795.

[2] Z. Gao, H. Li, H. Zhang, X. Liu, L. Kang, X. Luo, et al., PDTD: a web-accessible protein database for drug target identification, BMC Bioinformatics. 9 (2008) 104. doi:10.1186/1471-2105-9-104.

[3] A.L. Hopkins, C.R. Groom, The druggable genome, Nature Reviews Drug Discovery. 1 (2002) 727–730. doi:10.1038/nrd892.

[4] A. Altmann, P. Weber, D. Bader, M. Preuss, E.B. Binder, B. Müller-Myhsok, A beginners guide to SNP calling from high-throughput DNA-sequencing data, Hum. Genet. 131 (2012) 1541–1554. doi:10.1007/s00439-012-1213-z.

[5] C. Phillips, M. García-Magariños, A. Salas, A. Carracedo, M.V. Lareu, SNPs as Supplements in Simple Kinship Analysis or as Core Markers in Distant Pairwise Relationship Tests: When Do SNPs Add Value or Replace Well-Established and Powerful STR Tests? Transfus Med Hemother. 39 (2012) 202–210.

[6] J. Słodkowska, M.G. Rojo, Digital pathology in personalized cancer therapy, Folia Histochem. Cytobiol. 49 (2011) 570–578.

[7] M. Yu, Somatic mitochondrial DNA mutations in human cancers, Adv Clin Chem. 57 (2012) 99–138.

[8] A.H. Shih, O. Abdel-Wahab, J.P. Patel, R.L. Levine, The role of mutations in epigenetic regulators in myeloid malignancies, Nat Rev Cancer. 12 (2012) 599–612. doi:10.1038/nrc3343.

[9] X. Liang, J. Ma, H. Schatten, Q. Sun, Epigenetic changes associated with oocyte aging, Sci China Life Sci. 55 (2012) 670–676. doi:10.1007/s11427-012-4354-3.

[10] A. Nogueira da Costa, Z. Herceg, Detection of cancer-specific epigenomic changes in biofluids: powerful tools in biomarker discovery and application, Mol Oncol. 6 (2012) 704–715. doi:10.1016/j.molonc.2012.07.005.

[11] C. Nagy, G. Turecki, Sensitive periods in epigenetics: bringing us closer to complex behavioral phenotypes, Epigenomics. 4 (2012) 445–457. doi:10.2217/epi.12.37.

[12] S. Tyagi, F.R. Kramer, Molecular beacons: probes that fluoresce upon hybridization, Nat Biotechnol. 14 (1996) 303–308. doi:10.1038/nbt0396-303.

[13] S.A.E. Marras, S. Tyagi, F.R. Kramer, Real-time assays with molecular beacons and other fluorescent nucleic acid hybridization probes, Clin. Chim. Acta. 363 (2006) 48–60. doi:10.1016/j.cccn.2005.04.037.

[14] K. Wang, Z. Tang, C.J. Yang, Y. Kim, X. Fang, W. Li, et al., Molecular engineering of DNA: molecular beacons, Angew. Chem. Int. Ed. Engl. 48 (2009) 856–870. doi:10.1002/anie.200800370.

[15] K. Huang, A.A. Martí, Recent trends in molecular beacon design and applications, Anal Bioanal Chem. 402 (2012) 3091–3102. doi:10.1007/s00216-011-5570-6.

[16] D.M. Kolpashchikov, An elegant biosensor molecular beacon probe: challenges and recent solutions, Scientifica (Cairo). 2012 (2012) 928783–17. doi:10.6064/2012/928783.

[17] Z. Shen, S. Nakayama, S. Semancik, H.O. Sintim, Signal-on electrochemical Y or junction probe detection of nucleic acid, Chem. Commun. (Camb.). 48 (2012) 7580–7582. doi:10.1039/c2cc33280a.

[18] H. Asanuma, T. Osawa, H. Kashida, T. Fujii, X. Liang, K. Niwa, et al., A polycation-chaperoned in-stem molecular beacon system, Chem. Commun. (Camb.). 48 (2012) 1760–1762. doi:10.1039/c2cc16812j.

[19] C.-N. Yang, C.-Y. Hsu, Y.-C. Chuang, Molecular beacon-based half-adder and half-subtractor, Chem. Commun. (Camb.). 48 (2012) 112–114. doi:10.1039/c1cc14518e.

[20] Y. Kam, A. Rubinstein, A. Nissan, D. Halle, E. Yavin, Detection of endogenous K-ras mRNA in living cells at a single base resolution by a PNA molecular beacon, Mol. Pharmaceutics. 9 (2012) 685–693. doi:10.1021/mp200505k.

[21] A. Liu, Z. Sun, K. Wang, X. Chen, X. Xu, Y. Wu, et al., Molecular beacon-based fluorescence biosensor for the detection of gene fragment and PCR amplification products related to chronic myelogenous leukemia, Anal Bioanal Chem. 402 (2012) 805–812. doi:10.1007/s00216-011-5480-7.

[22] H. Yoshinaga, K. Nakano, N. Soh, T. Imato, AFM-imaging diagnosis method for single nucleotide polymorphism using molecular beacon DNA as an intramolecular ligation template of target DNA and a viewable indicator, Anal Sci. 28 (2012) 939–945.

[23] G. Qiao, Y. Gao, N. Li, Z. Yu, L. Zhuo, B. Tang, Simultaneous detection of intracellular tumor mRNA with bi-color imaging based on a gold nanoparticle/molecular beacon, Chemistry. 17 (2011) 11210–11215. doi:10.1002/chem.201100658.

[24] Y.-Q. Li, L.-Y. Guan, J.-H. Wang, H.-L. Zhang, J. Chen, S. Lin, et al., Simultaneous detection of dual single-base mutations by capillary electrophoresis using quantum dot-molecular beacon probe, Biosensors and Bioelectronics. 26 (2011) 2317–2322. doi:10.1016/j.bios.2010.10.002.

[25] K.A. Browne, Sequence-specific, self-reporting hairpin inversion probes, J. Am. Chem. Soc. 127 (2005) 1989–1994. doi:10.1021/ja046369w.

[26] Y. Kim, C.J. Yang, W. Tan, Superior structure stability and selectivity of hairpin nucleic acid probes with an L-DNA stem, Nucleic Acids Research. 35 (2007) 7279–7287. doi:10.1093/nar/gkm771.

[27] J. Grimes, Y.V. Gerasimova, D.M. Kolpashchikov, Real-time SNP analysis in secondary-structure-folded nucleic acids, Angew. Chem. Int. Ed. Engl. 49 (2010) 8950–8953. doi:10.1002/anie.201004475.

[28] C. Nguyen, J. Grimes, Y.V. Gerasimova, D.M. Kolpashchikov, Molecular-beacon-based tricomponent probe for SNP analysis in folded nucleic acids, Chemistry. 17 (2011) 13052–13058. doi:10.1002/chem.201101987.

[29] P. Santangelo, N. Nitin, G. Bao, Nanostructured probes for RNA detection in living cells, Ann Biomed Eng. 34 (2006) 39–50. doi:10.1007/s10439-005-9003-6.

[30] W.J. Rhee, P.J. Santangelo, H. Jo, G. Bao, Target accessibility and signal specificity in live-cell detection of BMP-4 mRNA using molecular beacons, Nucleic Acids Research. 36 (2008) e30–e30. doi:10.1093/nar/gkn039.

[31] J.F. Hopkins, S.A. Woodson, Molecular beacons as probes of RNA unfolding under native conditions, Nucleic Acids Research. 33 (2005) 5763–5770. doi:10.1093/nar/gki877.

[32] Y.V. Gerasimova, A. Hayson, J. Ballantyne, D.M. Kolpashchikov, A single molecular beacon probe is sufficient for the analysis of multiple nucleic acid sequences, ChemBioChem. 11 (2010) 1762–1768. doi:10.1002/cbic.201000287.

[33] D.M. Kolpashchikov, A binary DNA probe for highly specific nucleic Acid

recognition, J. Am. Chem. Soc. 128 (2006) 10625–10628. doi:10.1021/ja0628093.

[34] Y.V. Gerasimova, D.M. Kolpashchikov, Detection of bacterial 16S rRNA using a molecular beacon-based X sensor, Biosensors and Bioelectronics. 41 (2013) 386–390. doi:10.1016/j.bios.2012.08.058.

[35] D.M. Kolpashchikov, Y.V. Gerasimova, M.S. Khan, DNA nanotechnology for nucleic acid analysis: DX motif-based sensor, ChemBioChem. 12 (2011) 2564–2567. doi:10.1002/cbic.201100545.

[36] E.M. Cornett, E.A. Campbell, G. Gulenay, E. Peterson, N. Bhaskar, D.M. Kolpashchikov, Molecular logic gates for DNA analysis: detection of rifampin resistance in M. tuberculosis DNA, Angew. Chem. Int. Ed. Engl. 51 (2012) 9075–9077. doi:10.1002/anie.201203708.

[37] T.J. Fu, N.C. Seeman, DNA double-crossover molecules, Biochemistry. 32 (1993) 3211–3220.

[38] V.V. Demidov, M.D. Frank-Kamenetskii, Two sides of the coin: affinity and specificity of nucleic acid interactions, Trends Biochem. Sci. 29 (2004) 62–71. doi:10.1016/j.tibs.2003.12.007.

[39] E.M. Cornett, M.R. O'Steen, D.M. Kolpashchikov, Operating Cooperatively (OC) sensor for highly specific recognition of nucleic acids, PLoS ONE. 8 (2013) e55919. doi:10.1371/journal.pone.0055919.

[40] J.J. Sanchez, C. Phillips, C. Børsting, K. Balogh, M. Bogus, M. Fondevila, et al., A multiplex assay with 52 single nucleotide polymorphisms for human identification, Electrophoresis. 27 (2006) 1713–1724. doi:10.1002/elps.200500671.

[41] J. Li, X.-J. Qi, Y.-Y. Du, H.-E. Fu, G.-N. Chen, H.-H. Yang, Efficient detection of secondary structure folded nucleic acids related to Alzheimer's disease based on junction probes, Biosensors and Bioelectronics. 36 (2012) 142–146. doi:10.1016/j.bios.2012.04.003.

[42] S.V. Balasingham, T. Davidsen, I. Szpinda, S.A. Frye, T. Tønjum, Molecular diagnostics in tuberculosis: basis and implications for therapy, Mol Diagn Ther. 13 (2009) 137–151. doi:10.2165/01250444-200913030-00001.

[43] S. Hiyari, K.M. Bennett, Dental diagnostics: molecular analysis of oral biofilms, J Dent Hyg. 85 (2011) 256–263.

[44] M. Moschioni, W. Pansegrau, M.A. Barocchi, Adhesion determinants of the Streptococcus species, Microb Biotechnol. 3 (2010) 370–388. doi:10.1111/j.1751-7915.2009.00138.x.

[45] E.M. Starke, J.C. Smoot, J.-H. Wu, W.-T. Liu, D. Chandler, D.A. Stahl, Saliva-based diagnostics using 16S rRNA microarrays and microfluidics, Ann. N. Y. Acad. Sci. 1098 (2007) 345–361. doi:10.1196/annals.1384.007.

[46] D.P. Chandler, G.J. Newton, J.A. Small, D.S. Daly, Sequence versus structure for the direct detection of 16S rRNA on planar oligonucleotide microarrays, Appl. Environ. Microbiol. 69 (2003) 2950–2958.

[47] S. Lane, J. Evermann, F. Loge, D.R. Call, Amplicon secondary structure prevents target hybridization to oligonucleotide microarrays, Biosensors and Bioelectronics. 20 (2004) 728–735. doi:10.1016/j.bios.2004.04.014.

[48] J. Elbaz, O. Lioubashevski, F. Wang, F. Remacle, R.D. Levine, I. Willner, DNA computing circuits using libraries of DNAzyme subunits, Nature Nanotech. 5 (2010) 417–422. doi:10.1038/nnano.2010.88.

[49] L. Qian, E. Winfree, Scaling up digital circuit computation with DNA strand displacement cascades, Science. 332 (2011) 1196–1201. doi:10.1126/science.1200520.

[50] L. Qian, E. Winfree, J. Bruck, Neural network computation with DNA strand displacement cascades, Nature. 475 (2011) 368–372. doi:10.1038/nature10262.

[51] D.Y. Zhang, G. Seelig, Dynamic DNA nanotechnology using strand-displacement reactions, Nature Reviews Drug Discovery. 3 (2011) 103–113. doi:10.1038/nchem.957.

[52] J. Macdonald, D. Stefanovic, M.N. Stojanovic, DNA computers for work and play, Sci. Am. 299 (2008) 84–91.

[53] A. Lake, S. Shang, D.M. Kolpashchikov, Molecular Logic Gates Connected through DNA Four-Way Junctions, Angew. Chem. Int. Ed. 49 (2010) 4459–4462. doi:10.1002/anie.200907135.

[54] Y.V. Gerasimova, D.M. Kolpashchikov, Connectable DNA Logic Gates: OR and XOR Logics, Chem. Asian J. 7 (2011) 534–540. doi:10.1002/asia.201100664.

[55] Multidrug and extensively drug-resistant TB (M/XDR-TB): 2010 global report on surveillance and response. , World Health Organization, 2010.

[56] L.J. Abu-Raddad, L. Sabatelli, J.T. Achterberg, J.D. Sugimoto, I.M. Longini, C. Dye, et al., Epidemiological benefits of more-effective tuberculosis vaccines, drugs, and diagnostics, Proc. Natl. Acad. Sci. U.S.a. 106 (2009) 13980–13985. doi:10.1073/pnas.0901720106.

[57] T.S. Jordan, P.D. Davies, Clinical tuberculosis and treatment outcomes, Int. J. Tuberc. Lung Dis. 14 (2010) 683–688.

[58] R. Loddenkemper, D. Sagebiel, A. Brendel, Strategies against multidrug-resistant tuberculosis, Eur Respir J Suppl. 36 (2002) 66s–77s.

[59] J.J. Ellner, The emergence of extensively drug-resistant tuberculosis: a global health crisis requiring new interventions: Part II: scientific advances that may provide solutions, Clin Transl Sci. 2 (2009) 80–84. doi:10.1111/j.1752-8062.2008.00086.x.

[60] A. Jindani, G.E. Griffin, Challenges to the development of new drugs and regimens for tuberculosis, Tuberculosis. 90 (2010) 168–170. doi:10.1016/j.tube.2010.03.006.

[61] V. Donnabella, F. Martiniuk, D. Kinney, M. Bacerdo, S. Bonk, B. Hanna, et al., Isolation of the gene for the beta subunit of RNA polymerase from rifampicin-resistant Mycobacterium tuberculosis and identification of new mutations, Am. J. Respir. Cell Mol. Biol. 11 (1994) 639–643. doi:10.1165/ajrcmb.11.6.7946393.

[62] S. Morris, G.H. Bai, P. Suffys, L. Portillo-Gomez, M. Fairchok, D. Rouse, Molecular mechanisms of multiple drug resistance in clinical isolates of Mycobacterium tuberculosis, J. Infect. Dis. 171 (1995) 954–960.

[63] R. Blakemore, E. Story, D. Helb, J. Kop, P. Banada, M.R. Owens, et al., Evaluation of the analytical performance of the Xpert MTB/RIF assay, Journal of Clinical Microbiology. 48 (2010) 2495–2501. doi:10.1128/JCM.00128-10.

[64] P. Miotto, S. Bigoni, G.B. Migliori, A. Matteelli, D.M. Cirillo, Early tuberculosis treatment monitoring by Xpert(R) MTB/RIF, Eur. Respir. J. 39 (2012) 1269–1271. doi:10.1183/09031936.00124711.

[65] S. Armand, P. Vanhuls, G. Delcroix, R. Courcol, N. Lemaître, Comparison of the Xpert MTB/RIF test with an IS6110-TaqMan real-time PCR assay for direct detection of Mycobacterium tuberculosis in respiratory and nonrespiratory specimens, Journal of Clinical Microbiology. 49 (2011) 1772–1776. doi:10.1128/JCM.02157-10.

[66] D. Helb, M. Jones, E. Story, C. Boehme, E. Wallace, K. Ho, et al., Rapid detection of Mycobacterium tuberculosis and rifampin resistance by use of on-demand, near-patient technology, Journal of Clinical Microbiology. 48 (2010) 229–237. doi:10.1128/JCM.01463-09.

[67] S. Chakravorty, B. Aladegbami, M. Burday, M. Levi, S.A.E. Marras, D. Shah, et al., Rapid universal identification of bacterial pathogens from clinical cultures by using a novel sloppy molecular beacon melting temperature signature technique, Journal of Clinical Microbiology. 48 (2010) 258–267. doi:10.1128/JCM.01725-09.

[68] A. Troesch, H. Nguyen, C.G. Miyada, S. Desvarenne, T.R. Gingeras, P.M. Kaplan, et al., Mycobacterium species identification and rifampin resistance testing with high-density DNA probe arrays, Journal of Clinical Microbiology. 37 (1999) 49–55.

[69] A. Telenti, P. Imboden, F. Marchesi, D. Lowrie, S. Cole, M.J. Colston, et al., Detection of rifampicin-resistance mutations in Mycobacterium tuberculosis, Lancet. 341 (1993) 647–650.

[70] R.C. Cooksey, G.P. Morlock, S. Glickman, J.T. Crawford, Evaluation of a line probe assay kit for characterization of rpoB mutations in rifampin-resistant Mycobacterium tuberculosis isolates from New York City, Journal of Clinical Microbiology. 35 (1997) 1281–1283.

[71] H.H. El-Hajj, S.A. Marras, S. Tyagi, F.R. Kramer, D. Alland, Detection of rifampin resistance in Mycobacterium tuberculosis in a single tube with molecular beacons, Journal of Clinical Microbiology. 39 (2001) 4131–4137. doi:10.1128/JCM.39.11.4131-4137.2001.

[72] B. Malbruny, G. Le Marrec, K. Courageux, R. Leclercq, V. Cattoir, Rapid and efficient detection of Mycobacterium tuberculosis in respiratory and non-respiratory samples, Int. J. Tuberc. Lung Dis. 15 (2011) 553–555. doi:10.5588/ijtld.10.0497.

[73] N. Gous, L.E. Scott, E. Wong, T. Omar, W.D.F. Venter, W. Stevens, Performance of the Roche LightCycler real-time PCR assay for diagnosing extrapulmonary tuberculosis, Journal of Clinical Microbiology. 50 (2012) 2100–2103. doi:10.1128/JCM.00252-12.

[74] V. Vadwai, C. Boehme, P. Nabeta, A. Shetty, D. Alland, C. Rodrigues, Xpert MTB/RIF: a new pillar in diagnosis of extrapulmonary tuberculosis? Journal of Clinical Microbiology. 49 (2011) 2540–2545. doi:10.1128/JCM.02319-10.

[75] P.W.K. Rothemund, Folding DNA to create nanoscale shapes and patterns, Nature. 440 (2006) 297–302. doi:10.1038/nature04586.

[76] R.D. Barish, R. Schulman, P.W.K. Rothemund, E. Winfree, An information-bearing seed for nucleating algorithmic self-assembly, Proc. Natl. Acad. Sci. U.S.a. 106 (2009) 6054–6059. doi:10.1073/pnas.0808736106.

[77] J. Singh, R.C. Petter, T.A. Baillie, A. Whitty, The resurgence of covalent drugs, Nature Reviews Drug Discovery. 10 (2011) 307–317. doi:10.1038/nrd3410.

[78] M.H. Potashman, M.E. Duggan, Covalent Modifiers: An Orthogonal Approach to Drug Design, J. Med. Chem. 52 (2009) 1231–1246. doi:10.1021/jm8008597.

[79] S.G. Kathman, Z. Xu, A.V. Statsyuk, A Fragment-Based Method to Discover Irreversible Covalent Inhibitors of Cysteine Proteases, J. Med. Chem. 57 (2014) 4969–4974. doi:10.1021/jm500345q.

[80] P.A. Schwartz, P. Kuzmic, J. Solowiej, S. Bergqvist, B. Bolanos, C. Almaden, et al., Covalent EGFR inhibitor analysis reveals importance of reversible interactions to potency and mechanisms of drug resistance, Proc. Natl. Acad. Sci. U.S.a. 111 (2014) 173–178. doi:10.1073/pnas.1313733111.

[81] J. Singh, E. Evans, M. Hagel, M. Labinski, A. Dubrovskiy, M. Nacht, et al., Superiority of a novel EGFR targeted covalent inhibitor over its reversible counterpart in overcoming drug resistance, Med. Chem. Commun. 3 (2012) 780–4. doi:10.1039/c2md20017a.

[82] F. Esposito, A. Corona, E. Tramontano, HIV-1 Reverse Transcriptase Still Remains a New Drug Target: Structure, Function, Classical Inhibitors, and New Inhibitors with Innovative Mechanisms of Actions, Mol Biol Int. 2012 (2012) 586401. doi:10.1155/2012/586401.

[83] H. Huang, Structure of a Covalently Trapped Catalytic Complex of HIV-1 Reverse Transcriptase: Implications for Drug Resistance, Science. 282 (1998) 1669–1675. doi:10.1126/science.282.5394.1669.

[84] E. De Clercq, A 40-Year Journey in Search of Selective Antiviral Chemotherapy*, Annu. Rev. Pharmacol. Toxicol. 51 (2011) 1–24. doi:10.1146/annurev-pharmtox-010510-100228.

[85] R. Paredes, B. Clotet, Clinical management of HIV-1 resistance, Antiviral Research. 85 (2010) 245–265. doi:10.1016/j.antiviral.2009.09.015.

[86] M.-P. de Béthune, Non-nucleoside reverse transcriptase inhibitors (NNRTIs),

their discovery, development, and use in the treatment of HIV-1 infection: A review of the last 20 years (1989–2009), Antiviral Research. 85 (2010) 75–90. doi:10.1016/j.antiviral.2009.09.008.

[87] N. Apostolova, A. Blas-García, J.V. Esplugues, Mitochondrial interference by anti-HIV drugs: mechanisms beyond Pol-γ inhibition, Trends in Pharmacological Sciences. 32 (2011) 715–725. doi:10.1016/j.tips.2011.07.007.

[88] W. Lewis, B.J. Day, W.C. Copeland, Mitochondrial toxicity of NRTI antiviral drugs: an integrated cellular perspective, Nature Reviews Drug Discovery. 2 (2003) 812–822. doi:10.1038/nrd1201.

[89] W. Humphrey, A. Dalke, K. Schulten, VMD: visual molecular dynamics, J Mol Graph. 14 (1996) 33–8– 27–8.

[90] K. Vanommeslaeghe, E. Hatcher, C. Acharya, S. Kundu, S. Zhong, J. Shim, et al., CHARMM general force field: A force field for drug-like molecules compatible with the CHARMM all-atom additive biological force fields, J. Comput. Chem. 31 (2010) 671–690. doi:10.1002/jcc.21367.

[91] R.B. Best, X. Zhu, J. Shim, P.E.M. Lopes, J. Mittal, M. Feig, et al., Optimization of the additive CHARMM all-atom protein force field targeting improved sampling of the backbone φ, ψ and side-chain χ(1) and χ(2) dihedral angles, J Chem Theory Comput. 8 (2012) 3257–3273. doi:10.1021/ct300400x.

[92] W. Yu, X. He, K. Vanommeslaeghe, A.D. Mackerell, Extension of the CHARMM General Force Field to sulfonyl-containing compounds and its utility in biomolecular simulations, J. Comput. Chem. 33 (2012) 2451–2468. doi:10.1002/jcc.23067.

[93] K. Vanommeslaeghe, A.D. Mackerell, Automation of the CHARMM General Force Field (CGenFF) I: bond perception and atom typing, J. Chem. Inf. Model. 52 (2012) 3144–3154. doi:10.1021/ci300363c.

[94] K. Vanommeslaeghe, E.P. Raman, A.D. Mackerell, Automation of the CHARMM General Force Field (CGenFF) II: assignment of bonded parameters and partial atomic charges, J. Chem. Inf. Model. 52 (2012) 3155–3168. doi:10.1021/ci3003649.

[95] J.C. Phillips, R. Braun, W. Wang, J. Gumbart, E. Tajkhorshid, E. Villa, et al., Scalable molecular dynamics with NAMD, J. Comput. Chem. 26 (2005) 1781–1802. doi:10.1002/jcc.20289.

[96] A.G. Brown, D. Butterworth, M. Cole, G. Hanscomb, J.D. Hood, C. Reading, et

al., Naturally-occurring beta-lactamase inhibitors with antibacterial activity, J Antibiot. 29 (1976) 668–669.

[97] P.S. Saudagar, S.A. Survase, R.S. Singhal, Clavulanic acid: A review, Biotechnology Advances. 26 (2008) 335–351. doi:10.1016/j.biotechadv.2008.03.002.

[98] J. Llopis, J.M. McCaffery, A. Miyawaki, M.G. Farquhar, R.Y. Tsien, Measurement of cytosolic, mitochondrial, and Golgi pH in single living cells with green fluorescent proteins, Proceedings of the National Academy of Sciences. 95 (1998) 6803–6808.

[99] E.M. Cornett, Y.V. Gerasimova, D.M. Kolpashchikov, Two-component covalent inhibitor, Bioorganic & Medicinal Chemistry. 21 (2013) 1988–1991. doi:10.1016/j.bmc.2013.01.021.

[100] M.M. Hanna, S. Dissinger, B.D. Williams, J.E. Colston, Synthesis and characterization of 5-[(4-Azidophenacyl)thio]uridine 5'-triphosphate, a cleavable photo-cross-linking nucleotide analogue, Biochemistry. 28 (1989) 5814–5820.

[101] D.M. Kolpashchikov, N.I. Rechkunova, M.I. Dobrikov, S.N. Khodyreva, N.A. Lebedeva, O.I. Lavrik, Sensitized photomodification of mammalian DNA polymerase beta. A new approach for highly selective affinity labeling of polymerases, FEBS Letters. 448 (1999) 141–144.

[102] D.M. Kolpashchikov, T.M. Ivanova, V.S. Boghachev, H.P. Nasheuer, K. Weisshart, A. Favre, et al., Synthesis of base-substituted dUTP analogues carrying a photoreactive group and their application to study human replication protein A, Bioconjug. Chem. 11 (2000) 445–451. doi:10.1021/bc990102i.

[103] A. Wildfeuer, K. Räder, [Stability of beta-lactamase inhibitors and beta-lactam antibiotics in parenteral formulations as well as in body fluids and tissue homogenates. Comparison of sulbactam, clavulanic acid, ampicillin and amoxicillin], Arzneimittelforschung. 41 (1991) 70–73.

[104] A. Wildfeuer, K. Räder, Stability of beta-lactamase inhibitors and beta-lactam antibiotics in parenteral dosage forms and in body fluids and tissue homogenates: a comparative study of sulbactam, clavulanic acid, ampicillin and amoxycillin, International Journal of Antimicrobial Agents. 6 Suppl (1996) S31–4.

[105] A.R. English, J.A. Retsema, A.E. Girard, J.E. Lynch, W.E. Barth, CP-45,899, a beta-lactamase inhibitor that extends the antibacterial spectrum of beta-lactams: initial bacteriological characterization, Antimicrobial Agents and

Chemotherapy. 14 (1978) 414–419.

[106] J. Mulchande, L. Martins, R. Moreira, M. Archer, T.F. Oliveira, J. Iley, The efficiency of C-4 substituents in activating the beta-lactam scaffold towards serine proteases and hydroxide ion, Org. Biomol. Chem. 5 (2007) 2617–2626.

[107] S.V. Frye, The art of the chemical probe, Nature Chemical Biology. 6 (2010) 159–161. doi:10.1038/nchembio.296.